Industry
Canada
CRC

ANTENNA AMPLITUDE AND PHASE PATTERN MEASUREMENTS USING AN AIRCRAFT-TOWED TRANSMITTER (U)

by

Robert W. Jenkins

CRC REPORT NO. 95-003

September 1995
Ottawa

Canadä

Antenna Amplitude and Phase Pattern Measurements using an Aircraft-Towed Transmitter (U)

by

Robert W. Jenkins

Advanced Radio Systems Group
Radiocommunications Technologies Research

COMMUNICATION RESEARCH CENTRE, INDUSTRY CANADA
CRC REPORT NO. 95-003

Canada

September 1995
Ottawa

ABSTRACT

A previously-built antenna pattern measurement system, consisting of a short transmitting dipole and self-contained transmitter towed behind a light aircraft, was modified to permit measurements of both antenna gain and relative phase. A differential GPS positioning system was added to provide the necessaray accurate transmitter position information. The pattern measurement system is intended for calibrating HF antenna arrays used in direction-finding and other applications requiring knowledge of the array manifold.

The system was used to provide element pattern measurements on an HF antenna array located near Ottawa. The measurements provided a measure of the accuracy of the pattern measurement technique and its limits of applicability. The element patterns were observed to be affected by interactions between neighbouring elements and other localized features and, to a lesser extent, by larger-scale more distant ground or topographical effects.

RÉSUMÉ

On a modifié un dispositif pour mesurer le diagramme de rayonnement des antennes pour permettre a celui-ci de mesurer à la fois le gain et la phase relative. Le dispositif initial était constitué d'un dipole et d'un émetteur, le tout remorqué par un avion léger. Un dispositif GPS a été ajouté au dispositif initial afin de permettre l'acquisition de données précises sur la position de l'émetteur. Le dispositif amélioré de mesure de diagrammes de rayonnement d'antennes est destiné à la calibration de réseaux d'antennes HF utilisées en radiogoniométrie et autres applications pour lesquelles une connaissance de réseaux d'antennes est requise.

Le système fut utilisé pour l'obtention des diagrammes de rayonnement des éléments d'un réseau d'antennes situé près d'Ottawa. Ces mesures permirent de déterminer la précision de la technique de mesure des diagrammes de rayonnement et aussi de déterminer les limites d'application de la technique. Il fut observé que les diagrammes de rayonnement des éléments sont influencés par les interactions avec les éléments voisins, par les particularités topologiques du voisinage et à un moindre degré par les particularités topologiques lointaines à grande échelle.

EXECUTIVE SUMMARY

In order to address the need for calibrated HF antenna arrays for direction-finding and other applications, a previously-built antenna pattern measurement system (Xeledop) has been refurbished and modified to provide relative-phase as well as gain measurements. The Xeledop consists of a small transmitting dipole assembly towed behind a light aircraft. The transmitting dipole emits a tone at one of six frequencies, from 5 to 18 MHz. The transmitter location is provided by a differential global positioning system (GPS), with the master GPS receiver located aboard the aircraft, and another at a nearby ground reference location. A notebook computer on the aircraft records positions and provides the pilot with a display of the aircraft location relative to the intended flight path. Typical aircraft flight paths include circular paths at constant height, from which azimuthal patterns for fixed elevations may be found; and radial paths also at constant height, which are used to obtain elevation patterns at a fixed azimuth. The antenna array under calibration is required to provide a means of recording the received signals as well as maintaining timing with respect to the aircraft (GPS) position recording.

The Xeledop was used to measure the gain and relative-phase patterns of an HF antenna array near Ottawa, similar to one planned for direction-finding measurements in the arctic. The signals received by this array were reduced to audio frequencies where they were digitized and recorded. The recordings were Fourier analyzed to determine the exact frequency of transmission and the corresponding amplitude and phase of the signal at each antenna at that frequency. In this way, received Xeledop signals were measured with very high sensitivity by effectively restricting the signal measurements to a very narrow band, whose central frequency tracked that of the Xeledop thus compensating for any frequency drift or Doppler shift.

The refurbished Xeledop system was found to be capable of providing good gain and relative-phase patterns at elevation angles between 4.5° and 45°. The 4.5° lower limit was set by the increased region of ground contributing to the antenna response at low elevations, especially at lower radio frequencies, together with the limited distance away from the antenna array that the Xeledop can be flown at without exceeding the aircraft ceiling height (for any given elevation angle). The 45° upper limit was set mainly by small variations in the orientation of the towed transmitting dipole.

The pattern measurements showed that the HF antenna elements were affected by electrically coupled nearby conducting elements and local features external to the array, as well as more distant ground features. The electrically coupled localized effects dominated the azimuthal patterns at elevation angles of 11° and higher, while the ground effects were more important at the lowest elevation angle used (4.5°), especially at the lower HF frequencies.

Further work recommended in this area includes: numerical modelling of the antenna array to establish the degree to which the antenna patterns observed with the Xeledop agree with modelling predictions, and evaluating the effect of antenna gain errors on the direction-finding process.

TABLE OF CONTENTS

1.0 INTRODUCTION

Advances in digital signal processing technology have led to the implementation of sampled-aperture HF antenna arrays for various applications, including direction-finders, sky-wave and surface-wave HF radar, and adaptive-antenna interference cancellers. These systems often make use of the antenna pattern information, both amplitude and phase, in performing their function. In some cases (e.g., sparse-array direction-finding, adaptive antenna systems employing directional constraints) precise pattern information is required for successful operation.

HF antenna patterns are very sensitive to local conditions. Mutual coupling between the antennas in an array has a strong effect on their patterns. The nature of the ground, local inhomogeneities, and neighbouring structures all have significant effects. Seasonal and weather-related effects can be important, as the ground dampness, whether it is wet or frozen, and the possible existence of a layer of snow or ice, will influence the electrical constants of the ground and its reflection properties [1].

Ideally, the antenna patterns could be calculated from theory. However for most HF antenna applications, many of the relevant parameters are not known or can change with time. The ground parameters, local inhomogeneities, and neighbouring structures would all have to be measured. The detail and precision required in order to obtain reasonably accurate patterns is not clear; it varies with the local conditions as well as the application. In many cases, it may be more appropriate to conduct antenna pattern measurements more directly.

A CRC-built antenna pattern measurement system (Xeledop) was developed about 18 years ago, for measuring antenna gain patterns. This system consisted of a short transmitting dipole towed behind an aircraft. The received signal strength from the (ground-based) antenna of interest was recorded on a strip chart, along with time information. A portable radar system located near the ground-based antenna was used to determine the direction and distance to the aircraft. The radar data was also recorded and merged with the signal data in order to obtain the patterns. This system was used with considerable success to measure the antenna patterns of a number of communications antennas, both experimental and operational [2].

The Xeledop pattern measurement system has recently been refurbished, in order to address an HF direction-finding (DF) array calibration requirement. The added need for a phase (as well as amplitude) calibration required much more accurate position determination for the towed transmitter than was previously achieved with the portable radar. In order to accommodate this requirement and also modernize the data recording system at the same time, a differential GPS positioning system and a portable PC (for recording and displaying positions) were incorporated into the Xeledop. The refurbishment was designed and executed under contract by Petrie Telecommunications Ltd. of Ottawa. A report [3] provides a detailed description of the refurbished system.

In order to test the refurbished Xeledop pattern measurement system and gain experience in its use with direction-finding arrays, pattern measurements were carried out with a 12-element DF array installed outside Ottawa, near Leitrim. These tests were carried out with the assistance

of Petrie Telecommunications who flew the Xeledop transmitter and recorded the position information, and CSE who operated the DF array recording system and provided signal recordings.

The present report presents an overview of the Xeledop recording system and the results of the Leitrim pattern measurements. The results are interpreted both in terms of the Xeledop performance and its potential for measurements of this type, and the characteristics and predictability of the antenna patterns of the DF array.

2.0   THE XELEDOP PATTERN MEASUREMENT SYSTEM

The Xeledop pattern measurement technique is illustrated in Figure 1. The towed transmitting dipole radiates an HF tone which is received by the antenna array whose patterns are being determined. The received signals are recorded at the array, along with accurate time information. The aircraft location is determined by the differential GPS system, consisting of one GPS receiver at a ground-based reference location and a second receiver aboard the aircraft. A UHF
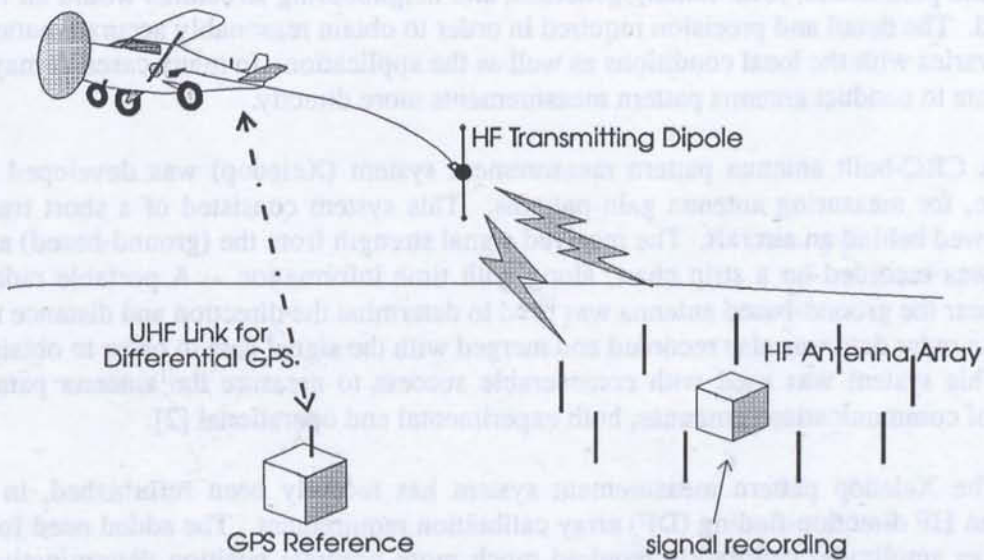
Figure 1. Xeledop pattern measurement system with differential GPS positioning.

radio link relays the ground-received GPS information to the aircraft, and position recording is performed on the aircraft. along with the GPS time. A correction is later made to the data for the fact that the Xeledop transmitter is located some distance behind and below the aircraft.

The rest of this section provides a brief description of the Xeledop equipment and its operation. Details can be found in the contractor's report [3].

2.1 Towed Xeledop Transmitter

Figure 2. Xeledop towed transmitter and towing assembly.

The Xeledop system is designed to be towed behind a Cessna 172 aircraft. Figure 2 provides a diagram (not to scale) of the towed transmitting unit and its towing assembly. The unit consists of a battery-powered HF trans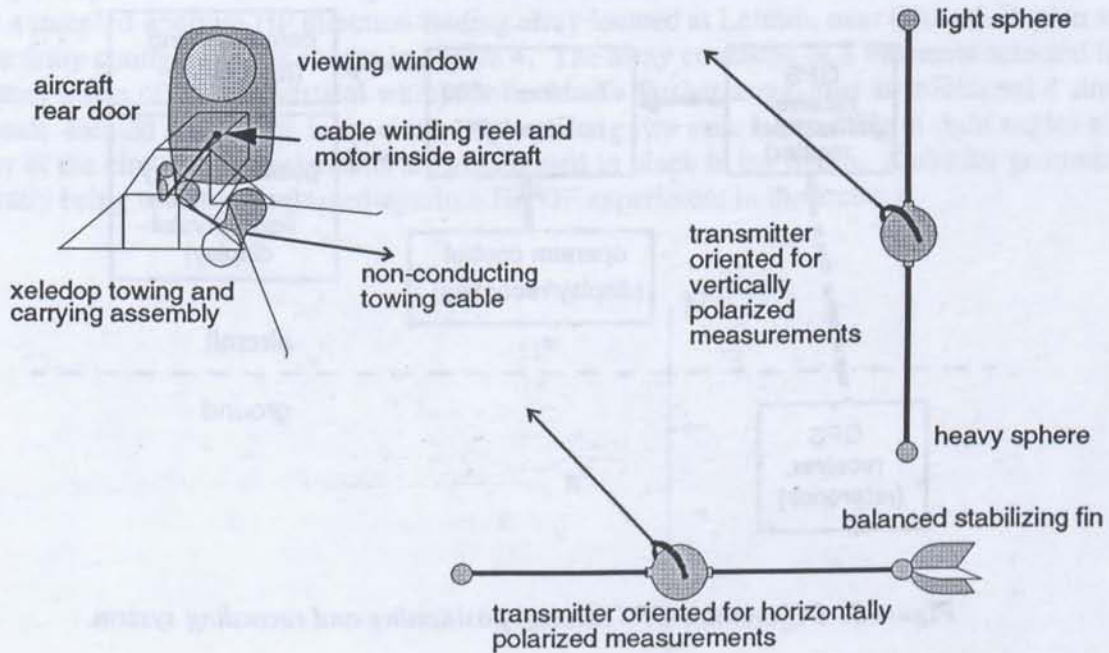mitter contained in a fibreglass sphere. Attached to the sphere are two conducting rods, each about 1.5m long, forming a short dipole antenna with the sphere at the center. A towing harness is attached to the sphere along an axis perpendicular to the dipole antenna, so that the transmitting unit is free to rotate about the harness axis. At the outer end of the dipole antenna are screw-on stabilizing units intended to maintain the antenna in either a vertical or horizontal position. For measurements requiring a vertically polarized transmission (i.e, the vertical position), the upper unit used is a small light sphere and the lower unit is a much heavier similar-size sphere. For horizontally polarized pattern measurements, the dipole antenna is maintained parallel to the path of travel of the aircraft (parallel to the air flow), with a small sphere attached at the front and a counterbalanced sphere and fin attached to the back.

Upon takeoff and landing, the transmitter unit is held tightly against the underside of the carrying assembly, by the tension in the (wound) non-conducting towing cable. Just before takeoff, the transmitter is started, and commences to run off its internal batteries. After takeoff, the towing cable is unwound from a motorized reel inside the aircraft door, so that the transmitter unit drops free of the carrying assembly and assumes its towed orientation behind and below the aircraft. Normally the transmitter is towed about 52 m behind and 25 m below the aircraft.

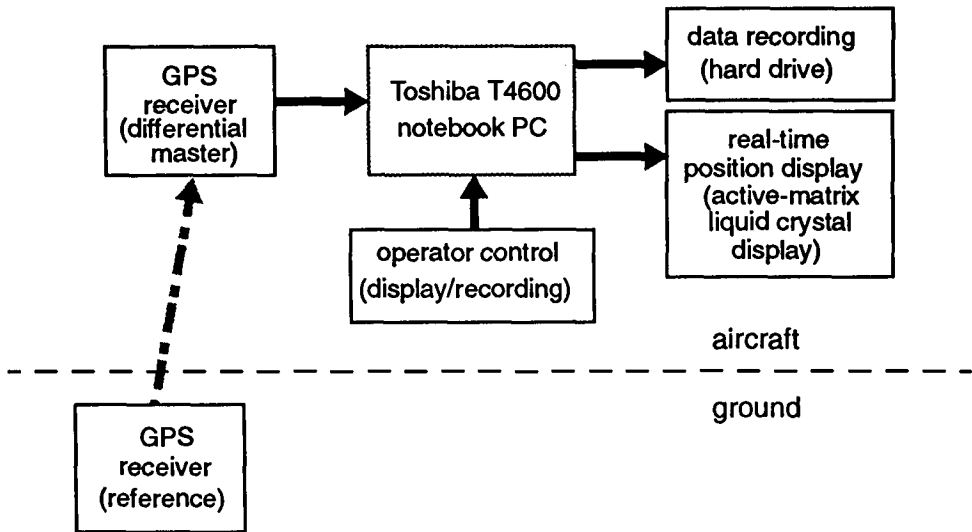## 2.2 Differential GPS Aircraft Position Determination System

Figure 3. Differential GPS aircraft positioning and recording system.

The differential GPS aircraft position determination system is illustrated in Figure 3. The reference receiver is located at a ground location whose geographic coordinates have been previously determined, by operating the GPS receiver in stand-alone mode for several days in order to obtain a good temporal average of the location. The location of the array to be measured is likewise determined from temporally averaged GPS measurements. During pattern measurement, the GPS signal information from the reference receiver is relayed to the master differential receiver located aboard the aircraft. The master receiver combines that information with the previously determined reference location to derive a GPS correction, which it applies to the aircraft position it had previously determined from the GPS signal received on the aircraft. The corrected aircraft position, along with the time and various GPS performance indicators, are recorded at one-second intervals in a file on the hard disk of a Toshiba T4600 notebook computer. After the measurements are completed, the position data file is transferred to a floppy disk for later analysis and merging with the signal information.

A program resident in the notebook computer provides a graphical display of the aircraft position relative to the antenna array of interest, to assist the pilot in staying close to the desired flight path. Typical runs include constant-height circular flight paths about the array and radial paths along a fixed azimuth relative to the array.

The Xeledop pattern measurement system does not include a system for recording the signals received by the antenna or array being calibrated. The candidate antenna or array is required to have its own signal recording system, including accurate timing information.

4

3.0 THE ANTENNA ARRAY AND SIGNAL RECORDING SYSTEM

The pattern measurement system was used to take measurements of the element responses from a sampled-aperture HF direction-finding array located at Leitrim, near Ottawa. A plan view of the array configuration is shown in Figure 4. The array consisted of 8 elements selected from the inner circle of 24 (6m vertical whip) elements of a Pusher array, plus an additional 4 similar elements located outside the inner circle in pairs along two axes intersecting at right angles at the center of the circle. These elements are highlighted in black in the figure. A similar geometry is currently being used for a sampled-aperture HF DF experiment in the arctic.
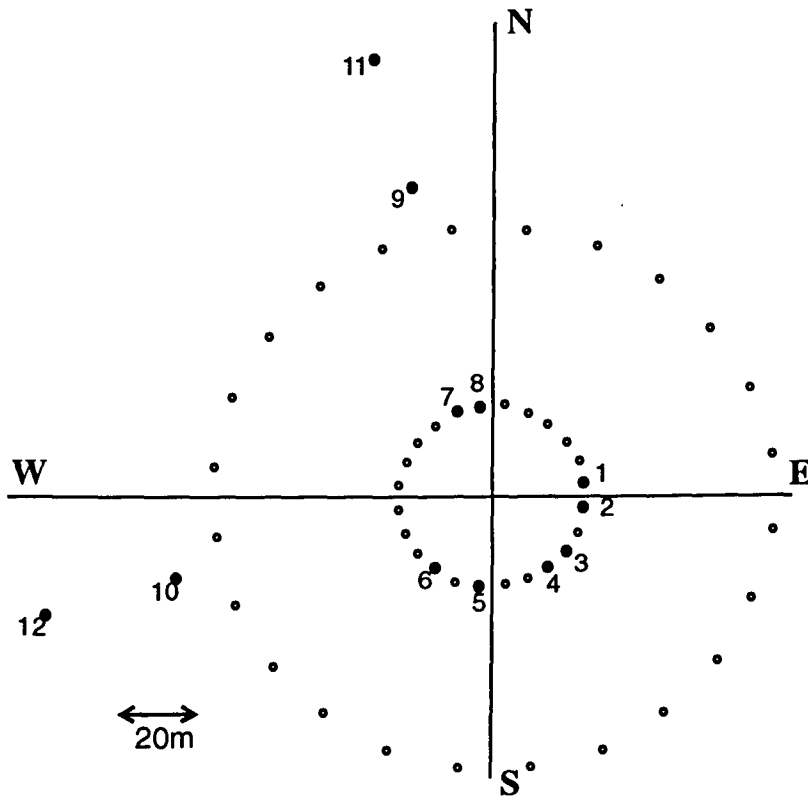
Figure 4. Plan view of receiving array being calibrated,
with sampled elements shown in black.

The signals from the array elements were fed through equal-length cables to commonly-tuned receivers, where they were reduced to near-baseband and sampled and digitized. The sampled-aperture signal recording system is shown in Figure 5. A digital sampling rate of approximately 10k samples/second was applied to the signals from each antenna. The samples from the 12 antennas were buffered into blocks of 12 x 8000 samples.
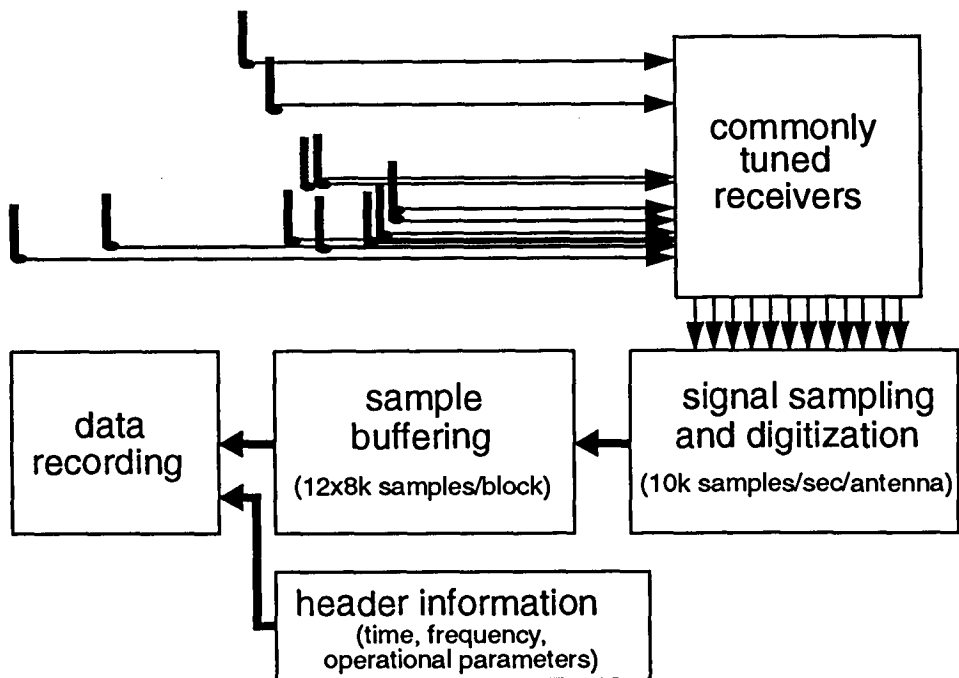
Figure 5. Sampled-aperture signal recording system.

The data were recorded on 2.3-Gbyte Exabyte tapes. Individual runs (i.e., continuous data recording sessions) were recorded as files. At the start of a run, a header record was placed on the tape, recording operational parameters including the receiver frequency, starting time and date, and receiver attenuation. The data blocks for the run were then written to tape as records, as they became ready.

The signal recording system was an experimental HF direction-finding and data recording system originally developed by MIT Lincoln Labs for sampled-aperture array development. A spectrum-analyzer display provided information on the channel occupancy in the vicinity of the Xeledop frequency, as well as a real-time display of the received Xeledop signal as a check that transmissions were being sent and received as expected.

An automated calibration measurement was performed on the receive array, in order to obtain the amplitude and phase response of each of the antenna channels. This was performed each day thata set of Xeledop flights was made. The resultant amplitude and phase responses were stored as complex amplitude correction factors in a separate file and recorded on floppy disk.

4.0 MEASUREMENT PLAN

In order to fully determine an antenna's radiation pattern, its gain and phase response must be obtained for all azimuths and elevations (i.e. all directions) of interest. A successful set of measurements will include the gain and phase response at enough specific directions that the response at other directions can be determined through an informed interpolation. Most antennas are intended for specific applications which may utilize less than the full range of possible directions. For example, the direction-finding antenna array under consideration is used to observe skywave signals whose path lengths are relatively long, and whose elevation angles are thus relatively low. Most elevation angles will be below 30°, and very few above 45°.

Theoretical antenna patterns are usually illustrated by fixing one direction parameter (e.g., elevation), and plotting the gain or phase response in terms of the other parameter (e.g., azimuth). The aircraft measurements are constrained by the possible paths that the aircraft can fly and the number of flights that can be economically made. Flying a constant-height circular flight path about the antenna(s) of interest results in a sequence of measurements that can be easily translated into an azimuthal pattern at a fixed elevation angle. Such flights are limited to elevation angles less than 50°, due to the ceiling altitude of the aircraft (about 6000 ft. for the Cessna 172 aircraft used in the measurements) and the minimum circular radius that the aircraft can accurately maintain. Flying a radial path provides a range of elevation angles at a constant azimuth; the result is a set of measurements that can be readily translated into an elevation pattern at a constant azimuth.

Table 1: Pattern measurement flight plan

Six frequencies: 5.1, 7.5, 9.3, 11.5, 15.1, and 18.0 MHz.

For each frequency:

azimuthal patterns (circular flight paths)
- 10 km radius, 3000 ft. altitude (~4.5° elevation), clockwise
- 7 km radius, 5000 ft altitude (~11° elevation), clockwise
- 7 km radius, 5000 ft altitude (~11° elevation), counterclockwise
- 5 km radius, 6000 ft altitude (~18° elevation), clockwise
- 3 km radius, 6000 ft altitude (~31° elevation), clockwise
- 2 km radius, 6000 ft altitude (~49° elevation), clockwise

elevation patterns (radial flight paths)
- 9 to 189° azimuth, 6000 ft altitude, from 10km to overhead to -10km ground distance
- 91 to 271° azimuth, 6000 ft altitude, from 10 km to overhead to -10 km ground distance

Table 1 lists the various runs that were attempted. In order to adequately cover the signal directions of interest, a set of circular paths were flown at various heights and circular radii, thus providing azimuthal patterns over the desired range of elevation angles. As a check on the measurements, one circular path was executed in both clockwise and counterclockwise directions. In addition two radial paths were flown, at right angles to each other.

5.0 DATA REDUCTION

The data reduction process is illustrated in Figure 6. It consists of interpreting and merging the aircraft position data and the recorded signal data, and then using the merged interpreted data to obtain the required antenna patterns. A set of C-language programs has been written to perform the data reduction on a Sun workstation.

```
┌─────────────┐                              ┌──────────────────┐
│ AIRCRAFT    │                              │ SIGNAL RECORDS   │
│ POSITION    │ ┌──────────┐                 │ (10k samples/    │
│ RECORDS     │ │ ANTENNA  │                 │  second          │
│ (lat, long, │ │ POSITIONS│                 │  for each        │
│ ht each     │ └──────────┘                 │  antenna)        │
│ second)     │                              └──────────────────┘
└─────────────┘
```
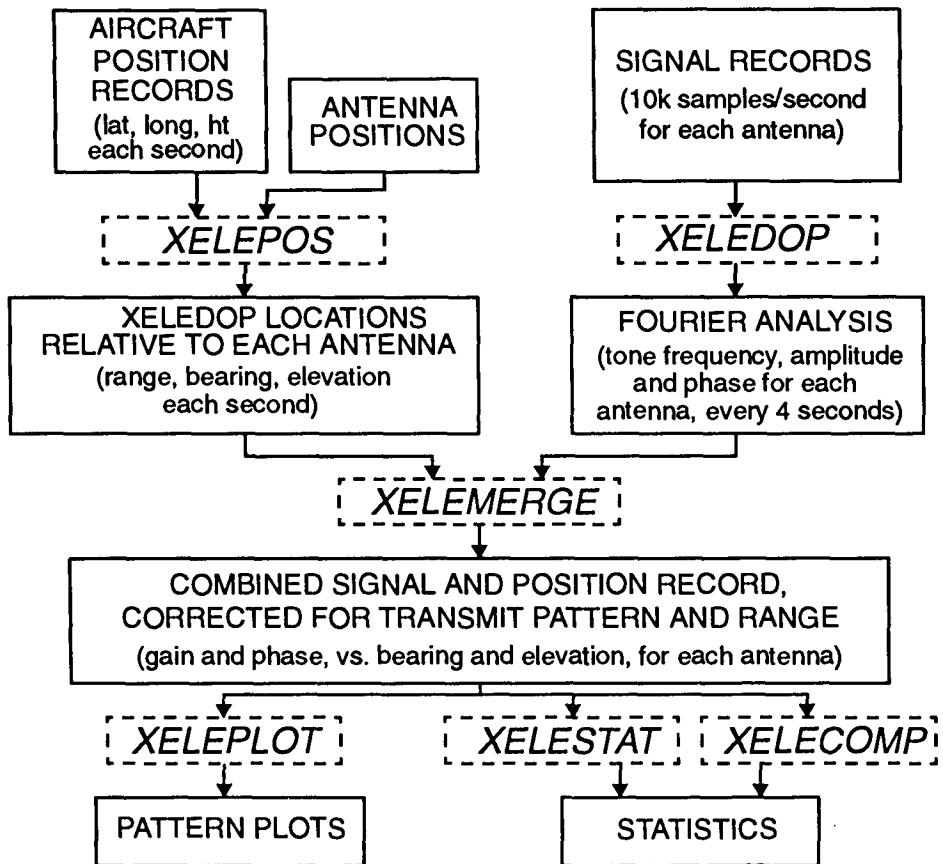
Figure 6. Data reduction.

5.1 Position Interpretation Program *XELEPOS*

The position interpretation program *XELEPOS* uses as input the aircraft position data provided by the differential GPS positioning system. This data consists of a file of time, geographical latitude, longitude, and height above sea level, and GPS quality indicators, recorded each second on the second. It also uses a file of additional information, including the antenna positions relative to the center of the array, the geographic coordinates of the array center, and the position of the towed transmitter behind and below the aircraft. From this information it creates a new file,

giving the bearing, elevation, and range of the towed transmitter for each antenna in the array, each second from the start to end of recording as before.

5.2 Signal Interpretation Program *XELEDOP*

The signal interpretation program *XELEDOP* takes as input the recorded signal data, which is read into and temporarily stored on a Sun workstation dedicated hard drive, one run at a time. (A single run can consume as much as 400 Mbytes of data storage.) The data reduction is computation-intensive and therefore very time-consuming. Steps have been taken to reduce the amount of computation and still obtain the desired results.

The program reads a block of signal samples (12 antennas x 8000 samples/antenna) at a time. Every 5th block of samples is used, resulting in a measurement roughly every 4 seconds.

The first step is determine the exact frequency of the transmitted Xeledop tone. The middle 1000 samples (out of 8000) for the first antenna are Fourier analyzed, and the frequency corresponding to the maximum signal strength selected. This frequency is selected as the 'central tone frequency', under the assumption that it corresponds to the transmitted Xeledop tone. Since the sample rate is approximately 10k samples/second, the frequency bins for a 1000-point Fourier analysis are 10 Hz wide.

The 8000 samples are then partitioned into 8 sub-blocks of 1000 samples each, and for each sub-block, the five Fourier components corresponding to the central tone frequency and the two frequencies on each side of the central tone frequency are found. Their powers are summed, to determine the total received signal strength in a bandwidth of 50 Hz about the frequency of maximum signal strength. The powers for the 8 sub-blocks are averaged, to obtain the mean received power for the block of samples which is then converted into an rms amplitude. This is done for each of the 12 antennas. The phase response of each antennas is found by vectorially adding the phasors (representing the amplitude and phase) found for the central tone frequency at each of the 8 sub-blocks, and taking the phase of the total. The antenna #1 phase is then subtracted from each of the antenna phases, so as to obtain a relative phase response.

The resultant rms amplitudes and relative phases for each of the 12 antennas are corrected for the channel response, given by the array calibration data, and written to file, along with the start time of the block and central tone frequency. This is repeated for every 5th block in the run.

5.3 Data Merging Program *XELEMERGE*

The data merging program *XELEMERGE* combines the interpreted position information, taken on a second-by-second basis with the interpreted signal information, recorded at approximate 4-second intervals. For each of the signal recording times, the positions are interpolated (in polar coordinates) so that the times match. This program is also used to remove any extraneous measurements due to interfering signals: the interpreted signal information is scanned by the

9

operator to determine if a single (or only slightly varying) frequency is seen for the whole run. Most of the time, other frequencies are occasionally seen as well. From this scan, the actual Xeledop frequency is determined. The *XELEMERGE* program is given the actual Xeledop frequency, and uses it to reject any blocks for which the central tone frequency is more than 100 Hz away.

The signal amplitudes are then corrected to a common range of 10 km. The transmitter antenna's elevation angle dependence of radiated power is corrected for, by using the cosine dependence given by theory for a short whip antenna in free space. The resultant normalized amplitudes are then converted to dB, and interpreted as relative gains. The result of the merging program is thus a file containing for each selected signal block in a particular run: a time, frequency, and for each of the 12 antennas, a transmitter range, azimuth, and elevation, a relative gain in dB, and a relative phase (relative to antenna#1). This file, along with those of the other runs, contains the results that make up the required antenna patterns.

5.4 Evaluation Programs *XELEPLOT*, *XELESTAT* and *XELECOMP*

Several programs have been written as interpretation aids.

The program *XELEPLOT* takes the merged results file for a run, and under operator control produces a file which the GNUPLOT public-domain plotting software can create plots from. Plots that can be created (and displayed or printed) in this manner include gain vs. azimuth and relative phase vs. azimuth (from circular-flight-path runs); and gain vs. elevation and relative phase vs. elevation (from radial-flight-path runs). The relative phase displays by themselves are not particularly illuminating. To facilitate interpretation of the phase data, *XELEPLOT* was modified to calculate the relative phase expected on the basis of a spherical wavefront for the transmitted Xeledop signal, and to plot the difference between observed and expected relative phase, as a function of either azimuth or elevation.

The program *XELESTAT* was written to calculate statistical results such as the rms and maximum difference from the average, in antenna gain over azimuth, or relative phase difference over azimuth. *XELECOMP* compares clockwise and counterclockwise runs at the same elevation angle, to determine the rms and maximum differences between the resultant amplitude and relative-phase-difference patterns.

6.0 RESULTS

6.1 Initial Results

The initial results included polar plots of antenna gain vs. azimuth, and rectilinear plots of the difference from a spherical wavefront in the relative antenna phase response $\Delta\phi$, vs. azimuth. Examples are shown in Figures 7 and 8.
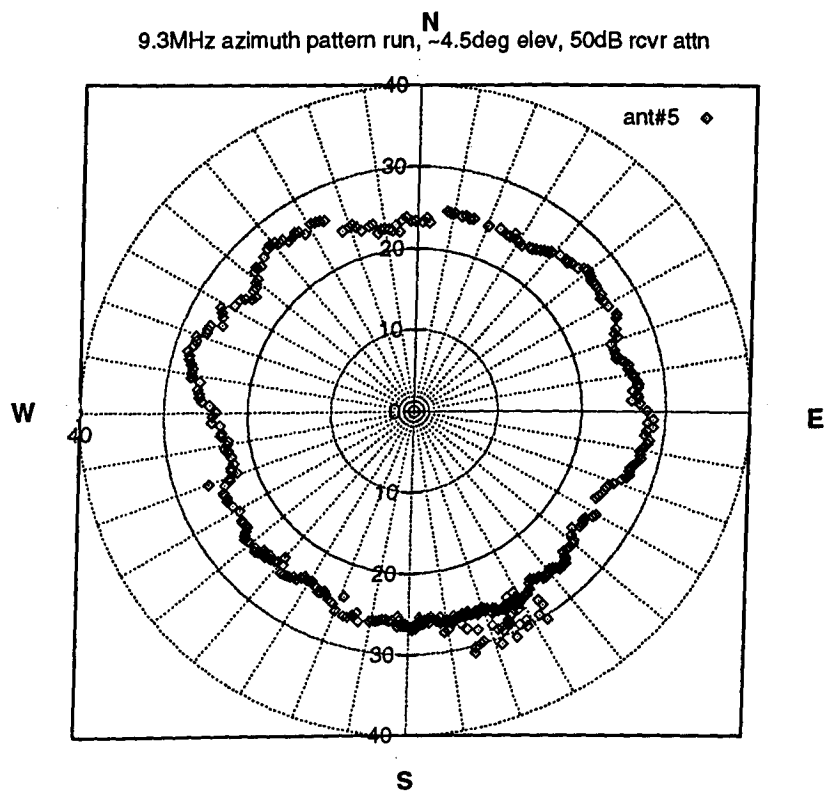
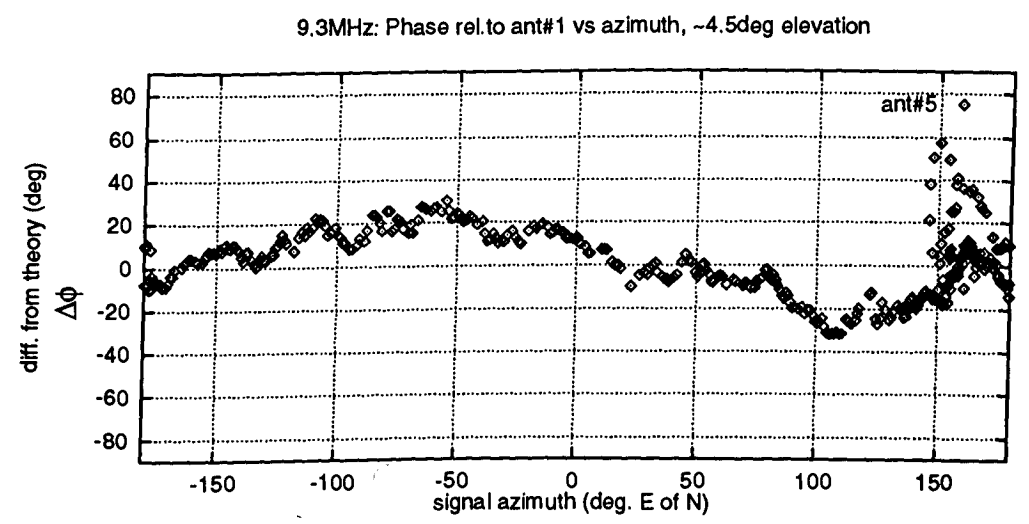*Figure 7. Representative initial plot of gain in dB, as a function of azimuth.*

Figure 8. Representative initial plot of relative phase difference Δφ, as a function of azimuth.

The azimuthal gain patterns were found to be circular within a few dB. The points taken near the start and end of the flight path, which overlap, were usually in good agreement, with occasional exceptions. These exceptions were related to the aircraft being off the constant-altitude circular flight path when recording was initiated or terminated.

The difference from theory ,$\Delta\phi$, in the relative phase response was expected to be close to zero degrees, with perhaps minor excursions as the aircraft changed azimuth. Instead, a roughly sinusoidal variation was found, having one cycle within the full 360° azimuth. Also, large differences were seen corresponding to times when the aircraft was moving away from a constant-radius circular path. In the example shown in Figure 9, the aircraft executed a tight circle off the flight path near the end of the run, at which time large differences were seen.

The sinusoidal behaviour in $\Delta\phi$ could not be readily explained by the antenna array itself or by its surroundings, leading one to suspect the measurement system. Several features of the sinusoidal behaviour may be seen in Figure 9. This figure shows the dependence of $\Delta\phi$ on azimuth for several different antennas, representing antenna separations of different sizes and baselines of different orientations. The separations and baseline orientations of the antennas of interest and the reference antenna (#1) can be seen in the plan view provided by Figure 4. The amplitude of the sinusoidal variation is seen to increase linearly with the separation between the two antennas. Also, the phase of the variation in $\Delta\phi$ is seen to depend on the orientation of the baseline. In the case of antenna pairs (#9, #1) and (#11, #1), the baselines are similarly oriented and the sinusoidal variation with azimuth is similar in its phase. However, the baseline for antenna pair (#5, #1) is roughly 100° ahead (in the clockwise sense), and the phase of its sinusoidal variation is likewise 100° ahead. It should be noted at this point that the aircraft was flying a clockwise circle about the array for these observations.

The amplitude of the sinusoidal variation in $\Delta\phi$ was observed to increase as the frequency was raised, and also as the radius of the circular flight path was decreased. This suggested that it was not real, but instead due to a discrepancy in the recorded position of the aircraft (and its towed transmitter) and the actual position corresponding to a given signal recording.

Probably the most suspicious feature of the initial results came from a comparison of the clockwise and counterclockwise flight path results that were made at an elevation of 11°. These results, in all cases, showed sinusoidal variations in $\Delta\phi$ that were 180° apart in their phase. The sinusoidal variations which changed with aircraft direction obviously could not be due to actual features of the antenna array being measured, but had to be an artifact of the measurement. Figure 10 shows the large relative phase differences measured for antenna pair (#11, #1) for both the clockwise and counterclockwise runs at ~11° elevation, at 9.3 MHz.

The observed sinusoidal variation of $\Delta\phi$ with azimuth can be explained by a discrepancy in the actual times recorded for the signal data and the position data. If approximately 8 seconds is subtracted from the 9.3-MHz signal-data times, so that the signal data is matched with position data 8 seconds earlier in the flight path than previously, the sinusoidal variation is seen to vanish. This corresponds to a position change of 300 m or more in the transmitter location. The most

likely cause of this recording error is in one of the systems (aircraft position or signal recording) not entering the GPS time, but instead a local time resident in the system computer. The actual reason for the time error has not been determined at the time of writing. A check on the signal

9.3MHz: Phase rel.to ant#1 vs azimuth, ~4.5deg elevation

antenna #5
40 m

9.3MHz: Phase rel.to ant#1 vs azimuth, ~4.5deg elevation

antenna #9
95 m

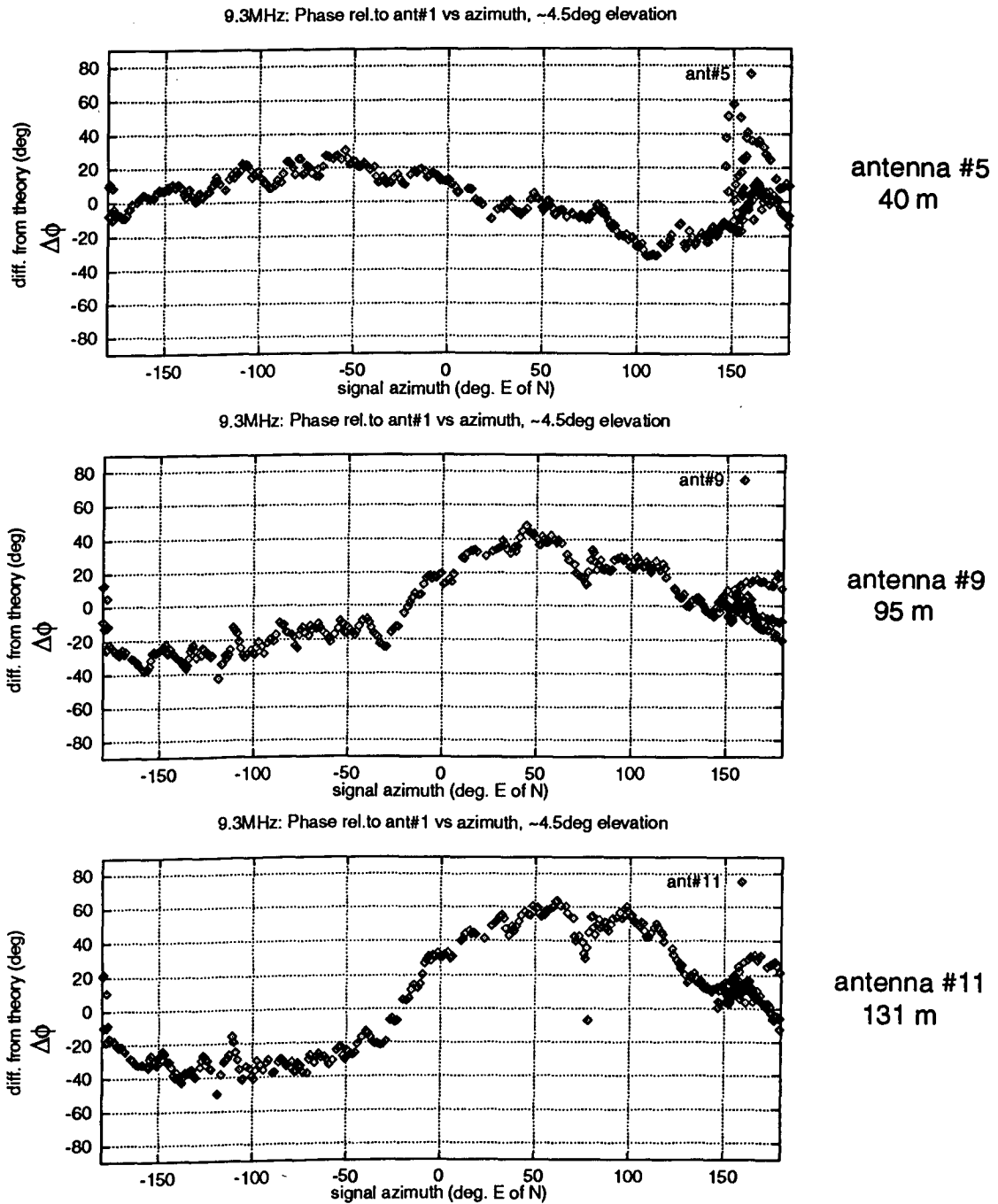**9.3MHz: Phase rel.to ant#1 vs azimuth, ~4.5deg elevation**

antenna #11
131 m

Figure 9. Initial plots of $\Delta\phi$ *vs. azimuth, for 3 different antenna separations, at 9.3 MHz.*

recording system when it was later installed at a northern location showed it to be recording correct time, to within a fraction of a second of the WWV time standard [4], and a later check on the GPS position-measuring system showed it to be recording correct time, to within a millisecond of the CHU time standard [5]. The discrepancy is thus not inherent to the equipment, but likely occured as a result of operator error in setting up for the calibration measurements.

9.3MHz: Phase rel.to ant#1 vs azimuth, ~11deg el., CW run

antenna #11
clockwise
flight path

9.3MHz: Phase rel.to ant#1 vs azimuth, ~11deg el., CCW run
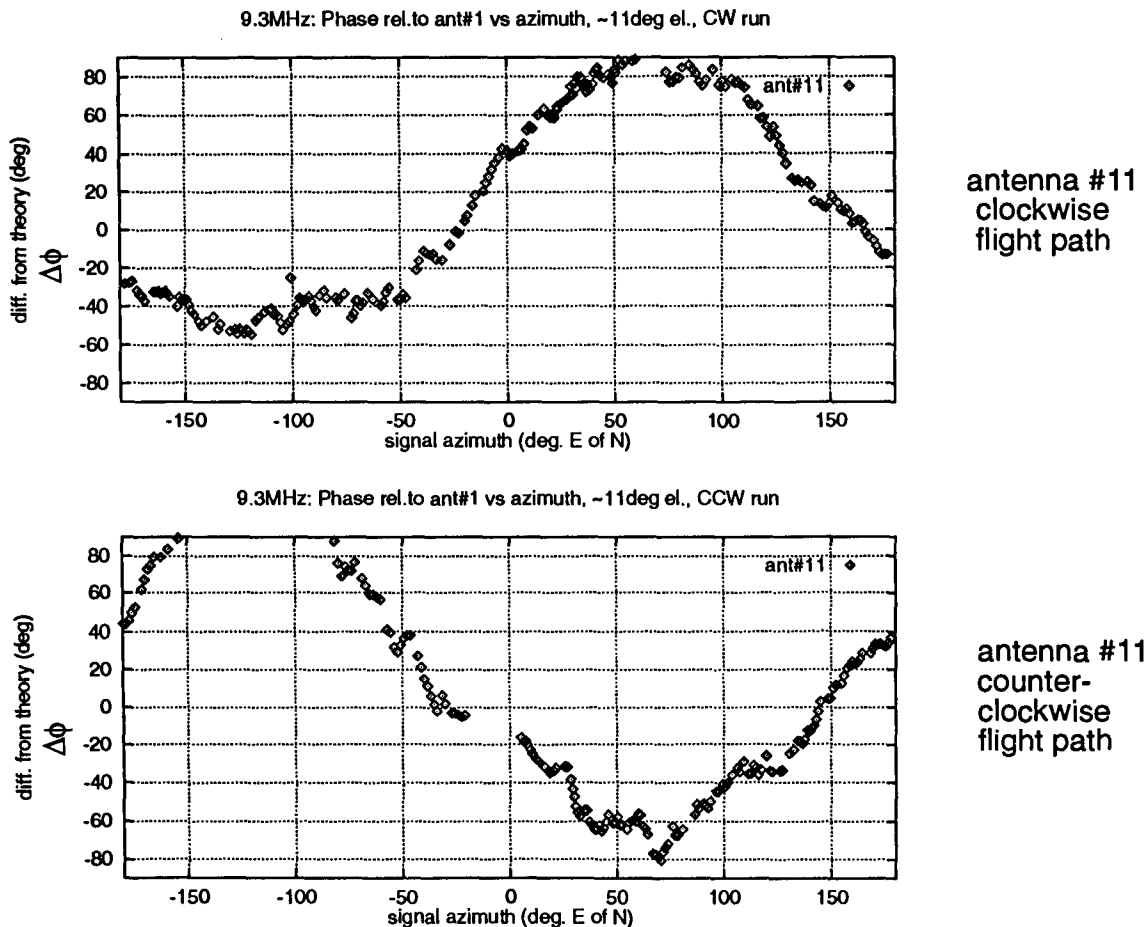

antenna #11
counter-
clockwise
flight path

Figure 10. Initial plots of $\Delta\phi$ vs. azimuth, for both clockwise and counterclockwise flight paths, for antenna #11, at ~11-deg. elevation and 9.3 MHz.

A trial-and-error procedure of correcting the signal recording times prior to merging the signal data with the position data was performed in order to find the most appropriate time correction (i.e., the correction that produced the best-matched clockwise and counterclockwise results). The correction was thus found to be -8.7 seconds for the 5.1-, 7.5-, 9.3-, and 11.5-MHz data taken between May 18 and June 10, 1994; and -9.8 seconds for the 15.1- and 18.0-MHz data taken on July 19 - 20, 1994.

Figure 11 shows the clockwise and counterclockwise azimuth patterns of relative phase difference $\Delta\phi$, found using this time correction. The large sinusoidal variations seen in Figure 10

14

have disappeared, and the two sets of measurements are in good agreement. Local variations from zero are similar in both measured patterns, giving weight to their existence as actual antenna-pattern features.

9.3MHz: Phase rel.to ant#1 vs azimuth, ~11deg el., CW run, -8.7s corr.

antenna #11
clockwise
flight path

9.3MHz: Phase rel.to ant#1 vs azimuth, ~11deg el., CCW run, -8.7s corr.
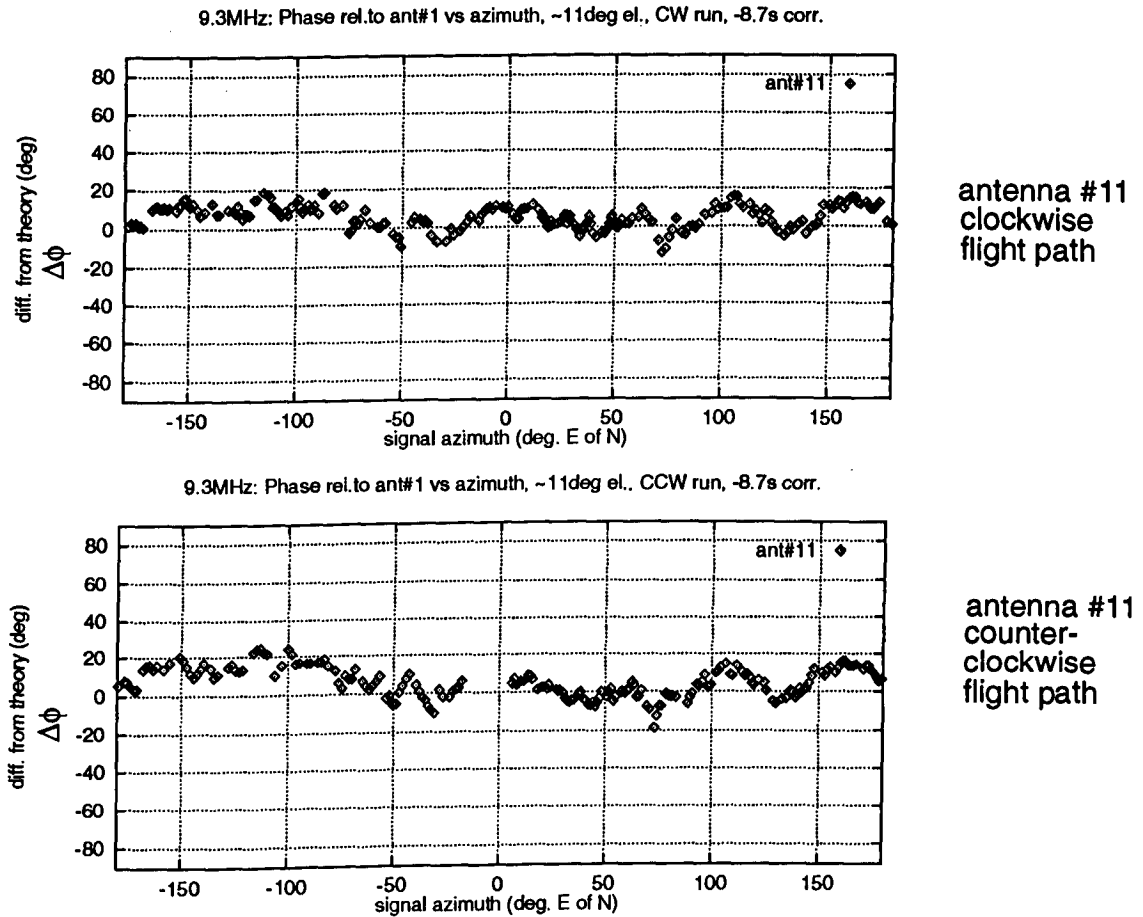
antenna #11
counter-
clockwise
flight path

Figure 11. Clockwise and counterclockwise flight-path patterns, of $\Delta\phi$ vs. azimuth, for antenna #11, at ~11-deg. elevation and 9.3 MHz, with a -8.7-second time correction applied to the signal data.

The remainder of the results discussed in this report have been corrected for the time discrepancy between position and signal recordings.

6.2 Gain Patterns

A typical set of azimuthal patterns is shown in Figure 12. This figure shows polar plots of gain vs. azimuth for antenna #5, located in the inner circle of the Pusher array. Plots are given for each of the elevation angles used in the flights. The operating frequency is 11.5 MHz.

15

4.5 deg. elevation

11 deg. elevation, CW

11 deg. elevation, CCW

18 deg. elevation
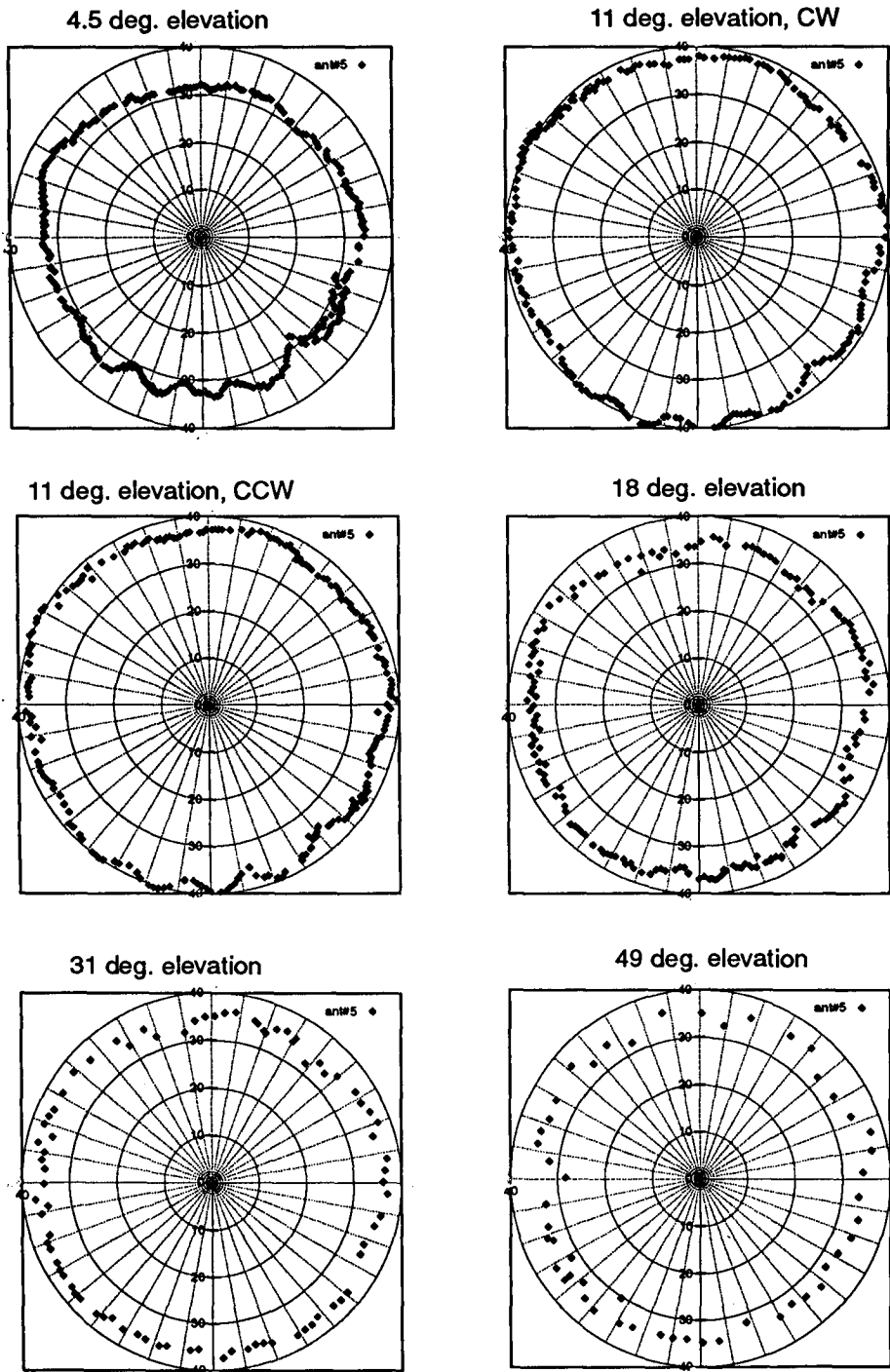
31 deg. elevation

49 deg. elevation

Figure 12. Azimuthal patterns of antenna gain in dB, for antenna #5 at 11.5-MHz operating frequency, and various elevation angles.

16

Several things are evident in Figure 12. The patterns are approximately circular, but there is some deviation away from circular with changes up to 6 dB occurring over azimuth. These changes are greatest at the lowest elevation, where the average antenna gain is reduced due to the undercutting caused by an imperfectly conducting ground. Changes in ground conductivity with azimuth are thus expected to cause greater azimuthal changes in gain at the lower elevation angles. As the elevation angle is increased, the changes in azimuth tend to retain their shape but become smaller. At the highest elevation angle (49°) the trend ceases, and the gains become scattered from point to point, likely due to time variations in the Xeledop transmitting antenna orientation. (More will be said about this later.) The reduced number of points at the higher elevation angles is due to the shorter time taken for the airplane to fly the smaller-radius circular flight path.

Figure 13 shows the corresponding elevation patterns obtained from the two nearly perpendicular radial flight paths, for antenna #5, at the same operating frequency. This result is typical of the results obtained.
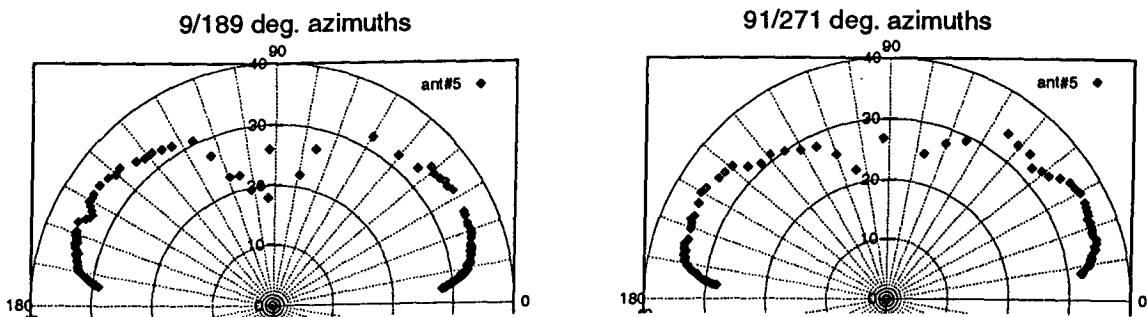

Figure 13. Elevation patterns of gain in dB, for antenna#5 at 11.5 MHz, taken on two near-perpendicular radial flight paths.

The elevation patterns, for elevation angles below 50°, are close to those expected for vertical whip antennas. The patterns are undercut at low angles (< 10°) due to the finite ground conductivity. A broad peak in gain exists between 10° and 45°. As the vertical is approached, the antenna gain drops towards zero (as expected from theory) with increasing scatter between points.

The very large scatter in the measured gains near 90° elevation is due to variations away from vertical in the Xeledop transmitting antenna orientation. Determining the gains from the observed signal strength involves multiplying the received amplitude by the reciprocal of the cosine of the elevation angle (i.e., the pattern of the short transmitting dipole). Therefore any deviations from vertical in the dipole orientation near 90° elevation (where this correction factor approaches infinity) will have a very large effect on the estimated gain. According to the contractor [3], the transmitting dipole moves away from its vertical orientation by up to 15° at most. This will cause errors in estimated gain of at most 1.8 dB at 30° elevation angle, 3 dB at 45°, and 5.7 dB at 60°. At 75° or above, the error in estimated gain can be extremely large.

17

At the highest elevation angle used for the azimuthal pattern measurements (49°), a maximum 15° variation from vertical in the Xeledop transmitting antenna orientation translates to potential errors in estimated gain from -2.0 dB to +3.5 dB. This is consistent with the variation in gain seen in the azimuthal gain patterns at 49°-elevation(e.g., Figure 12).

Figures 14, 15, and 16 show the azimuthal gain patterns found for several array elements at 11° elevation and the five operating frequencies. The gain patterns are unnormalized: the gains have been adjusted by fixed amounts so that the patterns found for the different frequencies occupy an approximately similar portion of a polar plot. Figure 14 gives the results for antenna #5, one of 24 elements located in the inner circle of the Pusher array; Figure 15, the results for antenna #9 located just outside the outer circle of the Pusher array; and Figure 16, the results for antenna #11 located well outside the Pusher array and away from other radiating elements. The positions of these antennas are shown in Figure 4.

An isolated vertical whip antenna on a homogeneous ground is expected to have a circular azimuthal pattern. Of the three antennas illustrated in Figures 14, 15, and 16, antenna#11 located well outside the Pusher array (and therefore well isolated from other conducting elements) has the most nearly-circular azimuthal patterns. The gain for this antenna, shown in Figure 16, remains within 1 dB of a perfect circle most of the time. The next-best behaved case shown in these figures is that of antenna #5 (Figure 14). This antenna is in the inner ring of the Pusher array and only 6.5 m away from other similar antennas. The case experiencing the greatest variation from a circular pattern is that of antenna #9 which is located about 15 m from a larger antenna in the outer ring of the pusher array. At 11° elevation, as illustrated in Figure 15, antenna #9 experiences azimuthal variations in gain from a constant (average) value, of typically 1 dB or more much of the time.

It can be seen from these figures that there is little similarity in the patterns found at the five different frequencies illustrated, for any particular antenna. This suggests that in order to obtain a complete set of measurements amenable to interpolation, it may be necessary to conduct measurements at substantially more frequencies than was done here.

Another point of comparison is the similarities that may be exhibited in the azimuthal patterns of the three antennas, at any frequency. An examination of Figures 14, 15, and 16 suggests some similarities, as well as significant differences. Firstly, the 5.1 MHz azimuthal patterns for all three antennas are very nearly circular, more so than those of the other three frequencies. At 9.3 MHz larger variations from circular occur, but the actual pattern shapes obtained for the three antennas differ considerably. At 11.5 MHz, the patterns are less circular, and again the pattern shapes obtained for the three antennas differ considerably. At 15.1 MHz, the patterns for the three antennas are more nearly circular, and as before, the variations with azimuth are different for the three antennas. At 18.0 MHz, the patterns for antennas #5 and #11 are nearly circular, but that of antenna #9 is distorted. These results suggest that at 11° elevation, localized features (nearby radiating elements and ground features) play a larger role than large-scale features (larger-scale ground and topological features) which affect the array as a whole, in determining the azimuthal patterns.

18

5.1 MHz

9.3 MHz

11.5 MHz

15.1 MHz

18.0 MHz

Figure 14. Unnormalized azimuthal patterns of antenna gain in dB, for antenna #5 at an approximate elevation of 11 degrees, for various receiving frequencies.

19

5.1 MHz

9.3 MHz

11.5 MHz

15.1 MHz

18.0 MHz

Figure 15. Unnormalized azimuthal patterns of antenna gain in dB, for antenna #9 at an approximate elevation of 11 degrees, for various receiving frequencies.

5.1 MHz

9.3 MHz

11.5 MHz

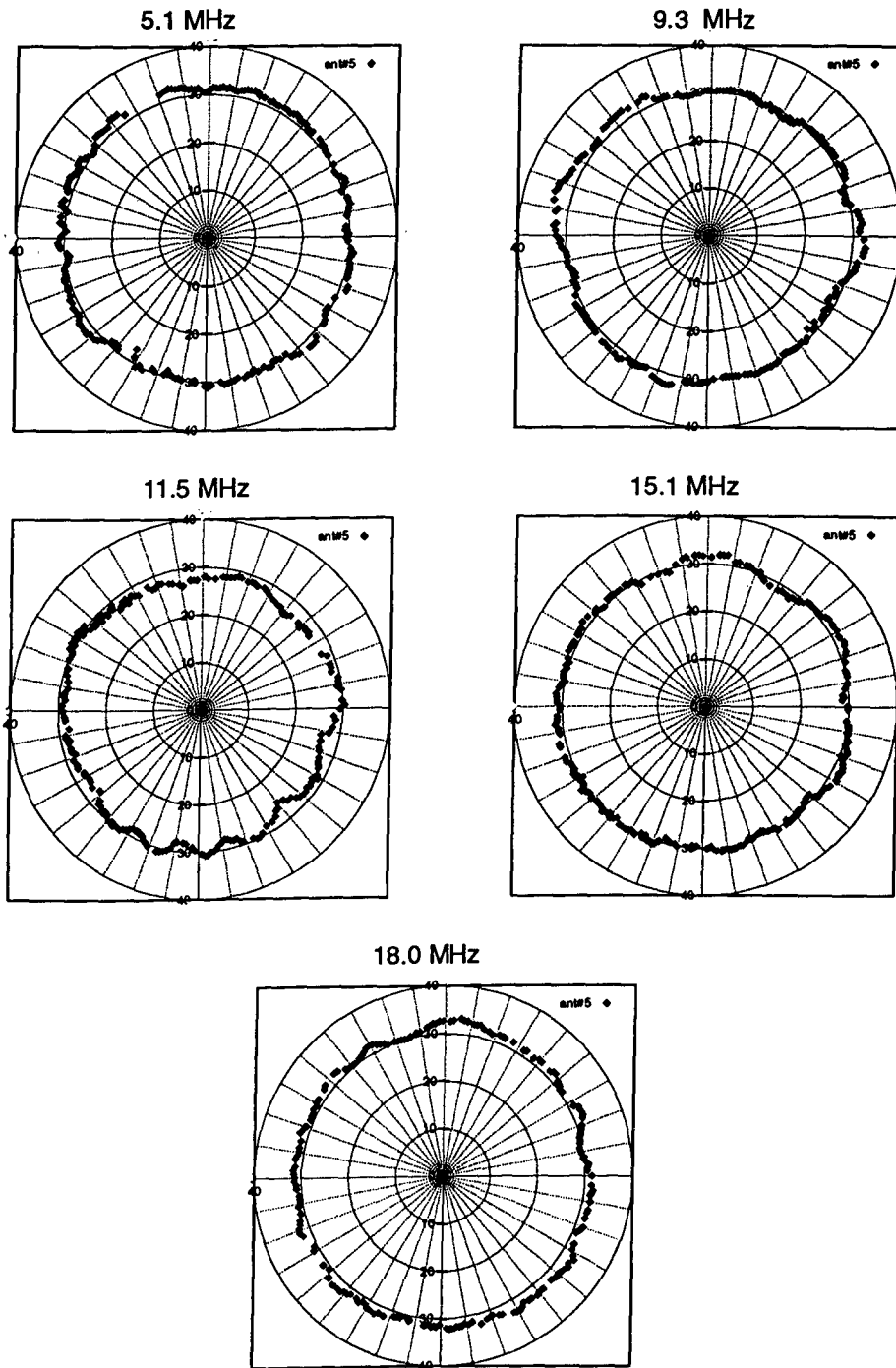**15.1 MHz**

18.0 MHz

Figure 16. Unnormalized azimuthal patterns of antenna gain in dB, for antenna #11 at an approximate elevation of 11 degrees, for various receiving frequencies.
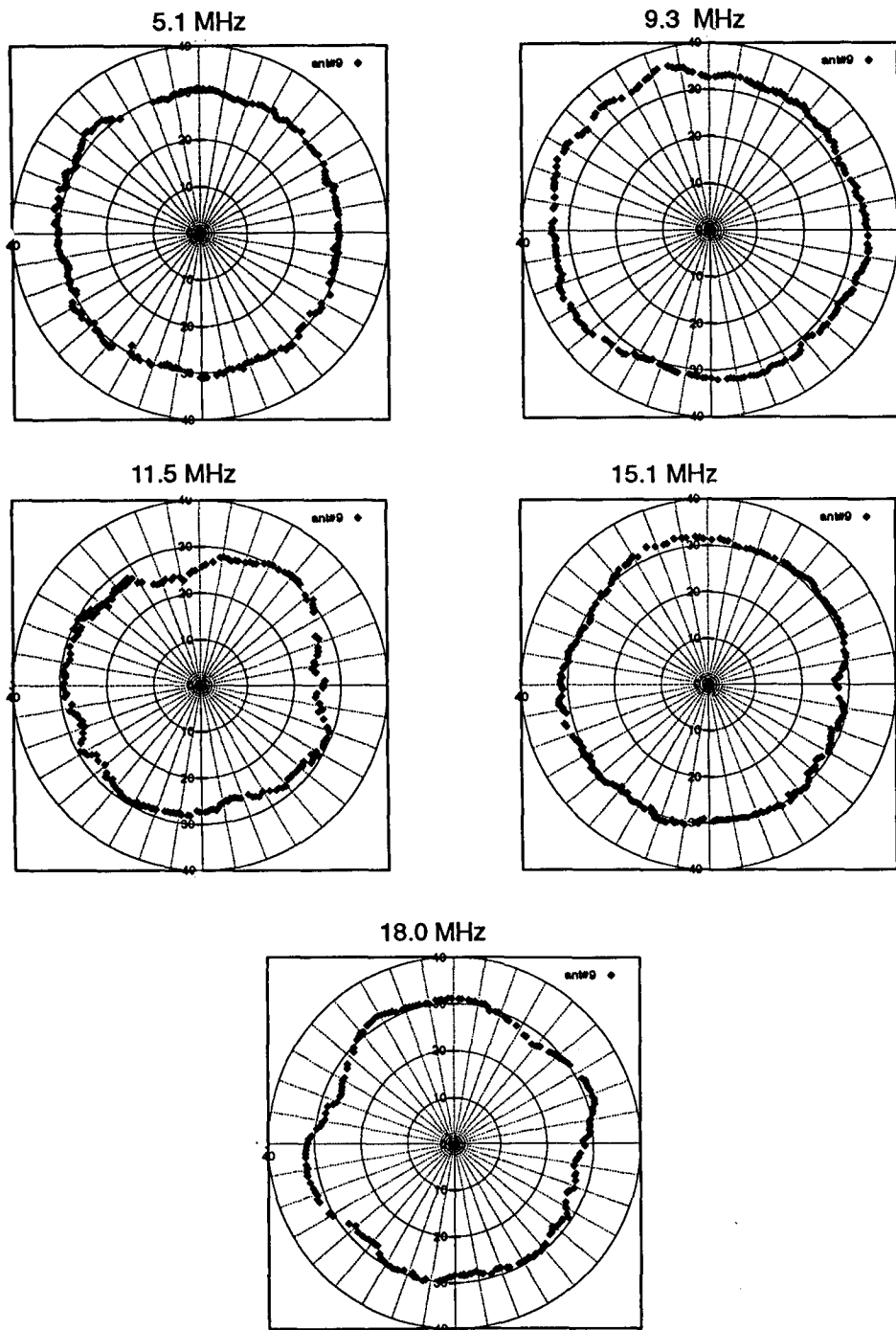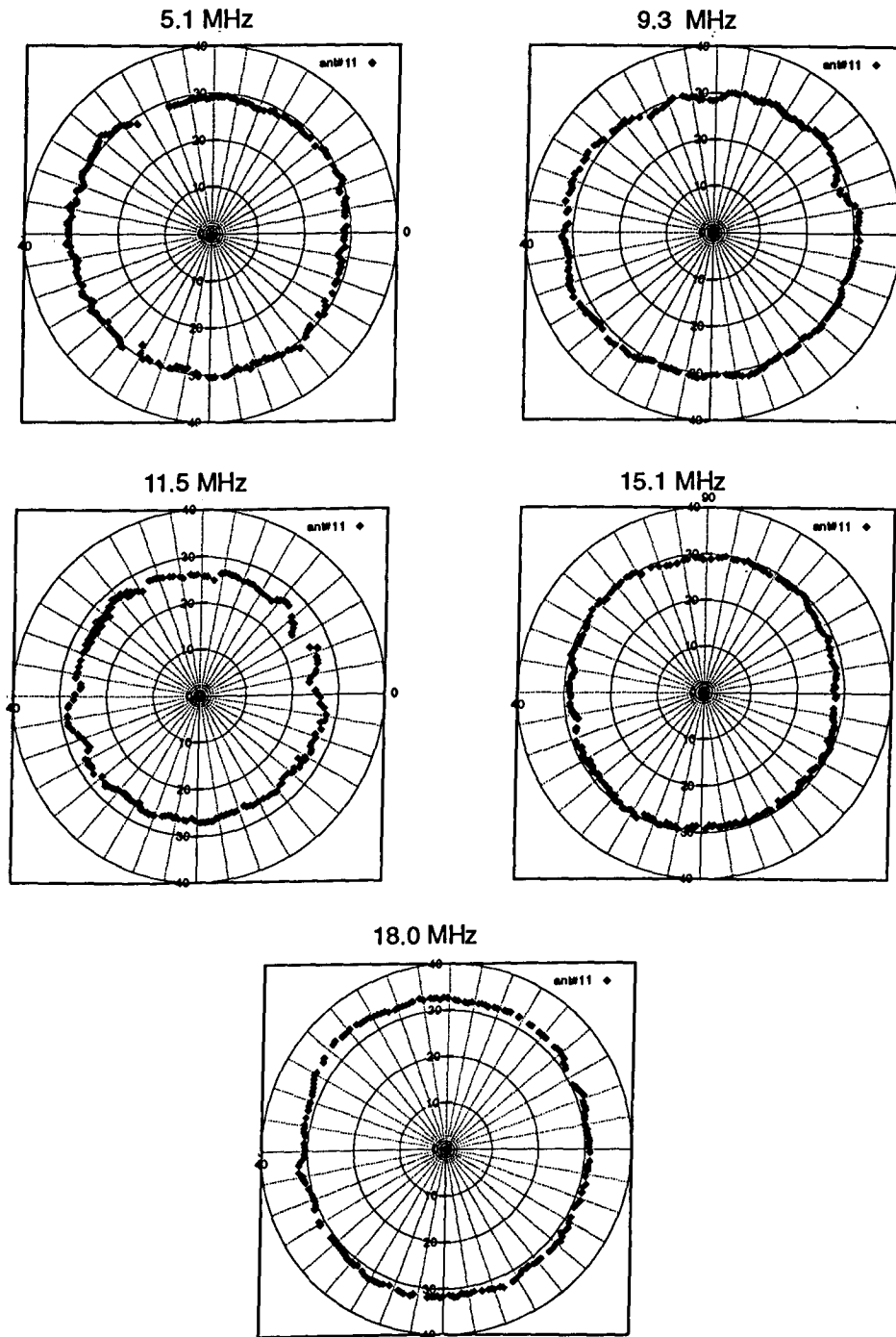
21

6.2.1 Effects of Local Features on Antenna Gain

The local features which affect antenna gain can be divided into two categories: those which are part of the antenna array itself including any supporting structures and ground radials; and those which are part of the external environment in the vicinity of individual elements.

The array features are expected to be nearly the same for each of the eight elements chosen from the inner circle of the array, since the additional four elements (which do interact differently with inner circle elements) are well-removed. These features should affect the patterns of the inner-circle elements in a similar way, once the patterns are rotated to reflect the position of each element in the inner circle.

By rotating the azimuthal patterns of each of the eight inner-circle elements (antennas 1 to 8 in Figure 4) by an amount corresponding to their location within the circle and then averaging them, it should be possible to observe the effect of the array features on the antenna patterns. External local features will be random with respect to the antenna position within the circle, and will tend to average out. The effect of large-scale more distant features (which have been noted in the previous section to be less important than those of local features) will also be reduced substantially by this procedure, since the element patterns are each rotated a different amount.

Figure 17 shows the average rotated azimuthal patterns thus obtained, along with the rotated pattern of antenna #5, for the 11° elevation angle run at each of the five frequencies. Both the azimuthal dependence introduced by the array features and the degree to which an individual antenna pattern is described by these features is evident in this figure.

At 5.1 MHz frequency, the average rotated pattern is almost independent of azimuth, and individual antenna-pattern azimuthal variations can be ascribed mainly to local external features. At 9.3 MHz, significant azimuthal variations begin to appear in the average rotated pattern, suggesting that array features are affecting the azimuthal dependence of the antenna patterns. Individual patterns follow the same azimuthal dependence as the average rotated pattern, with small variations which again can be attributed to local external features. The azimuthal dependence of the average rotated pattern is probably strongest at 11.5 MHz, suggesting that interacting array elements and other features play a strong role here. At 15.1 and 18.0 MHz, a significant azimuthal dependence is again noted for the average rotated pattern, with relatively small departures from the average pattern for individual antennas. Thus, the azimuthal patterns are affected by both array-related features and local external features, with the exception of the lowest frequency where the array-related features do not cause a significant azimuthal dependence.

Additional information is provided by Table 2 which gives the rms difference in gain from the average rotated patterns, over all measured azimuths, along with the rms variation from a mean azimuth-independent gain, for antennas #1 to 8. Rms variations from the average rotated pattern tend to decrease slightly with increasing frequency from approximately 0.8 dB at 5.1 MHz to 0.55 dB at 18.0 MHz. As previously noted, the average rotated pattern at 5.1 MHz is nearly independent of azimuth, and so the rms differences from the average pattern are about the same as

5.1 MHz

9.3 MHz

11.5 MHz

15.1 MHz

18.0 MHz
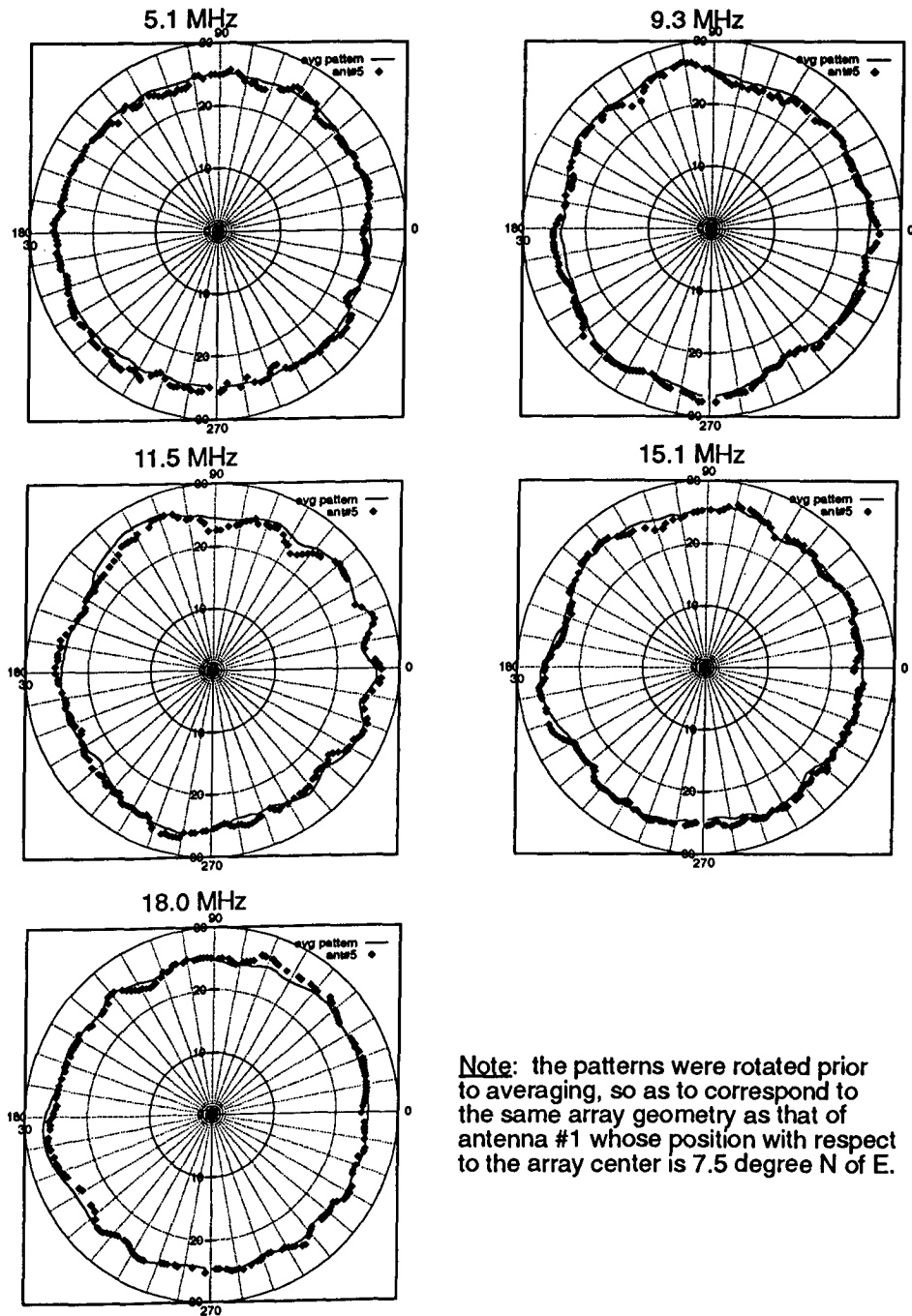
Note: the patterns were rotated prior to averaging, so as to correspond to the same array geometry as that of antenna #1 whose position with respect to the array center is 7.5 degree N of E.

Figure 17. Average azimuthal pattern of the inner-circle antennas #1-8, found by rotating individual patterns by an amount corresponding to the position in the circle so that the array geometry appears the same for all antennas, for an 11-degree elevation angle and the various operating frequencies, along with the rotated pattern for antenna #5.

the rms differences from a constant gain. At the higher frequencies this is not so: the differences in gain from a constant (azimuth-independent) value are greater that those rms differences from the average rotated pattern, in keeping with the azimuth dependence of individual antennas being due in part to array-related effects as well as local external features.

Table 2: Rms differences from average rotated pattern gain over azimuth, for antennas #1-8 and different operating frequencies, along with the rms differences from constant gain (in brackets)

Antenna#	5.1 MHz	9.3 MHz	11.5 MHz	15.1 MHz	18.0 MHz
1	0.74 dB (0.94)	0.66 dB (1.16)	0.63 dB (1.34)	0.53 dB (0.73)	0.53 dB (0.89)
2	0.72 (0.98)	0.63 (1.22)	0.64 (1.25)	0.46 (0.76)	0.59 (0.85)
3	0.63 (0.98)	0.61 (1.02)	0.58 (1.00)	0.51 (0.81)	0.54 (0.95)
4	0.65 (0.96)	0.61 (0.99)	0.57 (1.18)	0.49 (0.82)	0.51 (0.86)
5	0.67 (0.87)	0.74 (1.07)	0.86 (1.13)	0.63 (0.77)	0.59 (0.73)
6	0.81 (0.83)	0.77 (1.10)	0.62 (1.20)	0.69 (0.95)	0.53 (0.76)
7	0.89 (0.81)	0.68 (1.07)	0.63 (1.13)	0.46 (0.91)	0.54 (0.95)
8	0.83 (0.84)	0.78 (1.14)	0.61 (1.23)	0.51 (0.81)	0.50 (0.90)

6.2.2 Ground Effects on Antenna Gain

The theory of ground effects on antenna patterns indicates that the ground within the first Fresnel zone has the major effect on the antenna gain in any one direction. At higher elevation angles, this Fresnel zone is smaller and closer to the antenna. Thus the finding for 11° elevation, that local features are more important than larger-scale more distant features affecting the array as a whole in determining individual antenna patterns, also applies to higher elevation angles as well.

At lower elevation angles, it was seen (Figure 13) that the antenna gains are reduced due

to an imperfectly conducting ground. Thus the antenna patterns will be more affected by ground parameters at lower elevation angles. In addition, the Fresnel zone at low elevation angles becomes very large. These considerations suggest that larger-scale more distant ground features and other topological features will become more important in determining the azimuthal patterns at lower elevation angles.

In order to facilitate an examination of this possibility, the azimuthal gain patterns found for the lowest elevation flight path (4.5° elevation) at the five operating frequencies are plotted in Figures 18, 19, and 20 for antennas #5, #9 and #11 respectively.

In order to interpret the results, it is useful to consider the extent of the first Fresnel zone (and thus the ground region that contributes to antenna gain). This is a function not only of elevation angle and to some extent the antenna height, but also the operating frequency. Table 3 gives the distance that the first Fresnel zone extends out from a short antenna, for the 4.5° elevation, for the frequencies used, and transmitters at several ground distances including the 10 km ground distance of the Xeledop transmitter flight path. It can be seen that the ground contributing to the antenna gain extends considerably further from the array at lower frequencies than higher ones.

Table 3: Extent of first Fresnel zone on ground, for a short antenna and a signal at 4.5° elevation.

frequency (MHz)	transmitter at 10 km ground distance	transmitter at 20 km ground distance	transmitter infinitely far away
5.1	4.9 km	6.5 km	9.5 km
9.3	3.4 km	4.2 km	5.2 km
11.5	3.0 km	3.5 km	4.2 km
15.1	2.4 km	2.8 km	3.2 km
18.0	2.1 km	2.4 km	2.7 km

From Figures 18, 19, and 20, it can be seen that for the lowest frequency (5.1 MHz), the azimuthal gain patterns for the three antennas are similar in that they all have a drop in gain by several dB, for azimuths between 0° and 90° (the north-east quadrant). At the next higher frequency (9.3 MHz), there is some evidence of slightly lower gains in this quadrant, but the similarities between antennas are less evident. At the higher frequencies (11.5, 15.1, and 18.0 MHz), the differences between the 4.5-elevation azimuthal gain patterns of the three antennas dominate, and little if any similarity is seen.

These observations, together with the Fresnel zone considerations of Table 3, suggest that the common ground feature affecting antenna gain is of large extent (since it affects a whole quad-

Figure 18. Unnormalized azimuthal patterns of antenna gain in dB, for antenna #5 at an approximate elevation of 4.5 degrees, for various receiving frequencies.

5.1 MHz

9.3 MHz

11.5 MHz

15.1 MHz

18.0 MHz

Figure 19. Unnormalized azimuthal patterns of antenna gain in dB, for antenna #9 at an approximate elevation of 4.5 degrees, for various receiving frequencies.

27

5.1 MHz

9.3 MHz
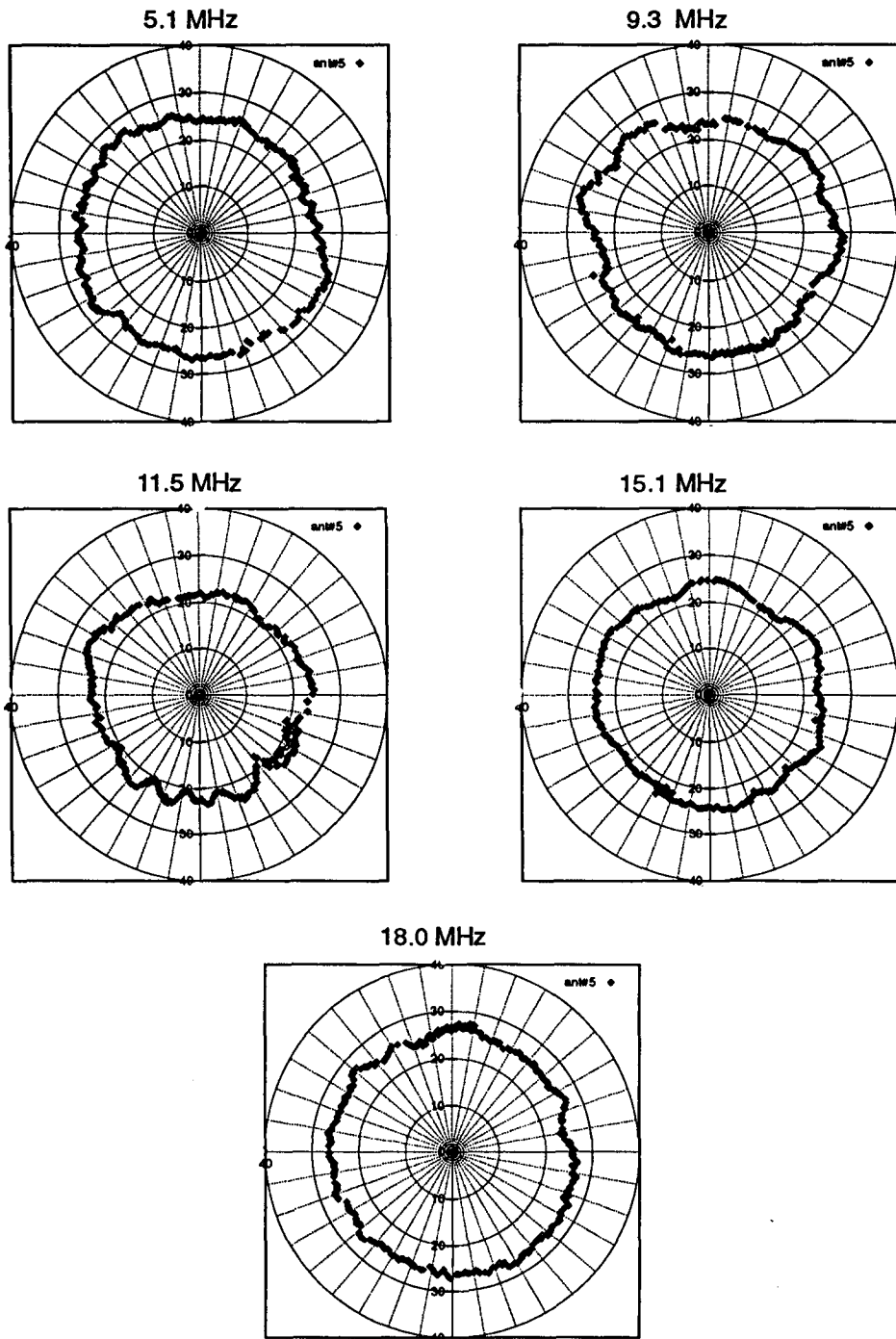

11.5 MHz

15.1 MHz

18.0 MHz

Figure 20. Unnormalized azimuthal patterns of antenna gain in dB, for antenna #11 at an approximate elevation of 4.5 degrees, for various receiving frequencies.
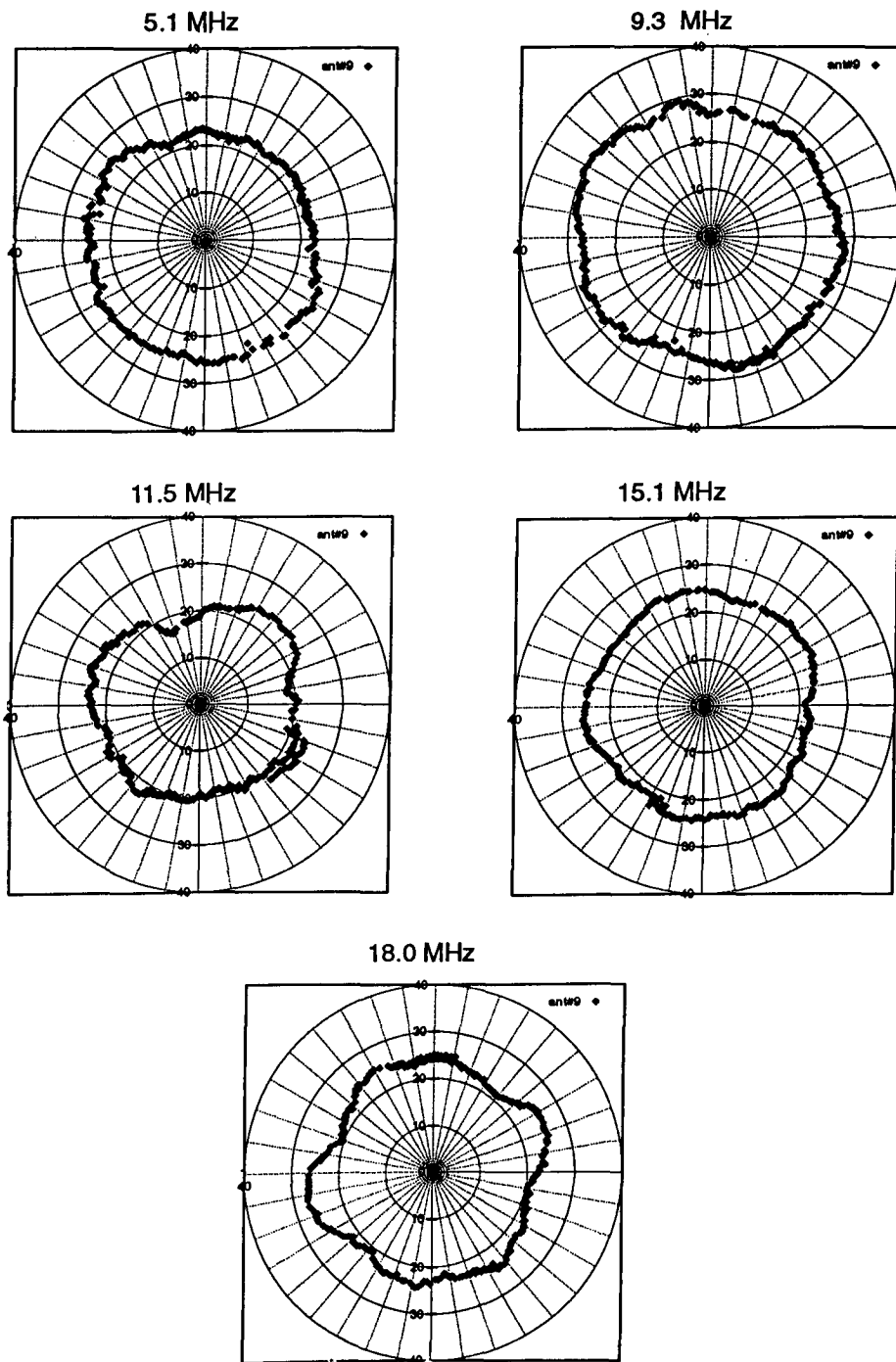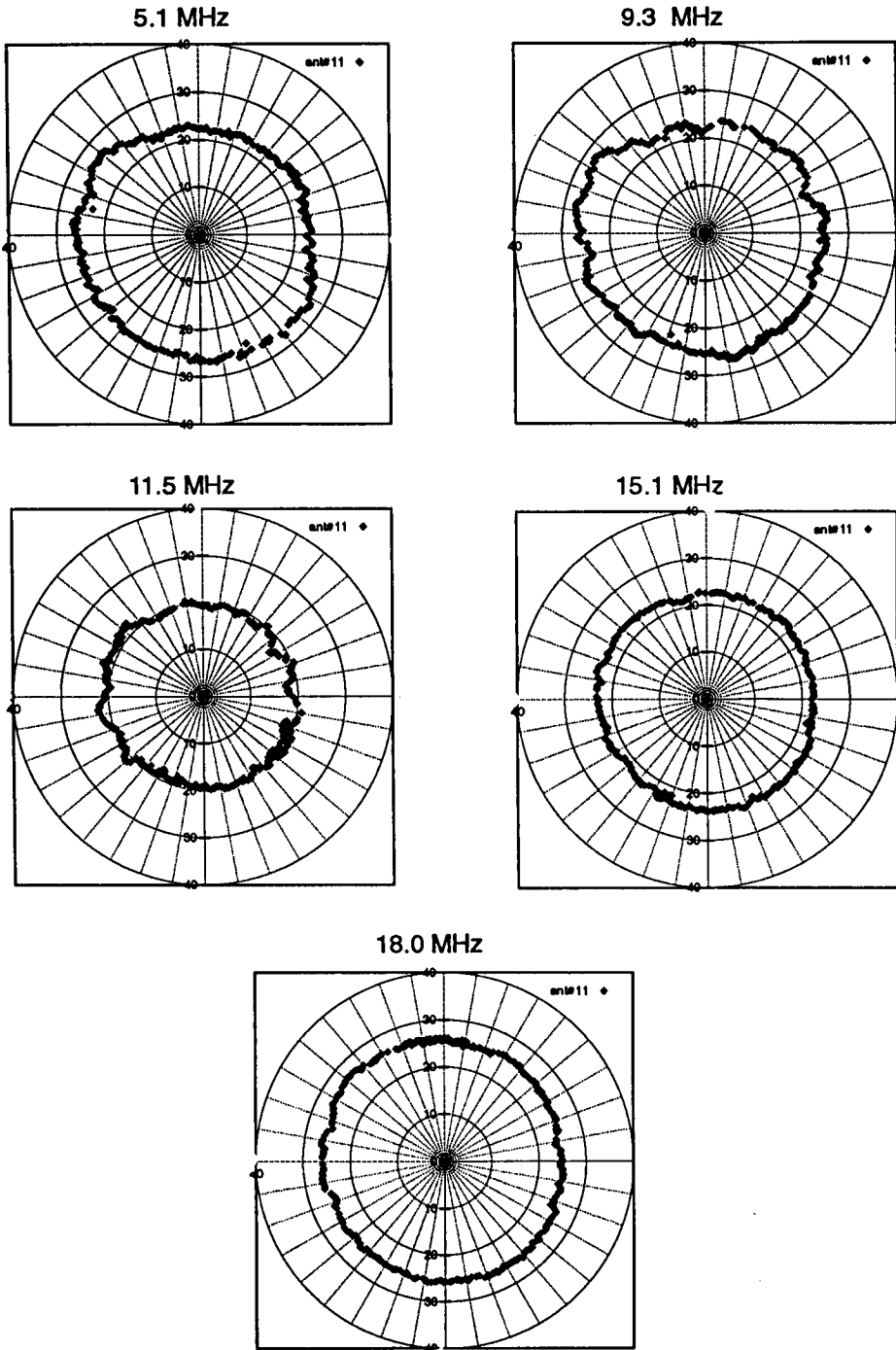
rant) and is situated outwards of 3 km from the receiving array in the north-east direction. (An inspection of available maps indicates a large marsh in that direction, extending outwards of 4 km from the array.) The lack of any clear similarities between antennas in their azimuthal gain patterns at higher frequencies or at higher elevation angles implies that there were no anomalous ground features 0.5 to 3 km away from the array that caused significant distortions to the array patterns. Ground anomalies within 0.5 km would affect the three antennas differently, and thus would not be distinguishable from other local features.

An examination of Table 3 raises another issue. It shows the extent of the first Fresnel zone, or ground affecting antenna gain, for transmitters at several distances, including the Xeledop flight path, and an infinitely far transmitter. The question is whether the Xeledop measurements yield antenna gains that are representative of the gains that will be experienced for the array when it is receiving much more distant (effectively infinitely far) skywave signals. From Table 3, the ground extent of the first Fresnel zone for the Xeledop measurements (10-km ground distance) is much less than the ground extent for skywave signals (infinite ground distance). At 5.1 MHz, it is only 0.5x that of skywave signals, while at 18.0 MHz, it is 0.8x that of the skywave value. Thus the gains measured at 4.5° elevation cannot be said to be truly representative of the skywave gains, especially at the lower frequencies.

In order to obtain more adequate measurements of low-elevation-angle gain, it is necessary to use larger radius flight paths. The largest practical radius for the 4.5° elevation is 20 km; this radius corresponds to an aircraft height of 6000 ft., near the maximum for light aircraft. From Table 3, the first Fresnel zone at a 20-km transmitter distance extends further than that for 10 km, to 0.7 of the skywave value at 5.1 MHz, and 0.9 that of the skywave value at 18.0 MHz. The 5.1-MHz value can be said to be marginally acceptable provided there is no dramatic change in the outer portion of the skywave Fresnel zone such as a change from shore to ocean water. Thus 4.5° elevation represents the lowest elevation that the Xeledop method can be used to obtain useful skywave antenna patterns at 5 MHz.

At higher elevation angles, the contributing ground regions (as expressed by the first Fresnel zone) are smaller, and for a given transmitter ground distance, more nearly the same as those for skywave signals. Table 4 lists the Fresnel zone extents for the next higher elevation angle of 11° (where the Xeledop flight path had a ground radius of 7 km.) From this table, it can be seen that the contributing ground regions are sufficiently close that the Xeledop measurements are representative of skywave signals. At the lowest frequency, 5.1 MHz, the first Fresnel zone for the Xeledop measurement extends out 0.83 times as far as the Fresnel zone for skywave signals. With the exception of a dramatic change in the ground conditions in the outer portion of the skywave Fresnel zone, the Xeledop measurement provides an adequate estimate of the skywave gains at this elevation angle. The Xeledop measurements at the higher elevation angles also provide an adequate measure of the skywave antenna gains.

Table 4: Extent of first Fresnel zone, for a short antenna and a signal at 11° elevation

frequency (MHz)	transmitter at 7-km ground distance	transmitter infinitely far away
5.1	1.22 km	1.46 km
9.3	0.72 km	0.80 km
11.5	0.60 km	0.65 km
15.1	0.46 km	0.50 km
18.0	0.39 km	0.41 km

6.2.3 Statistical Results

A way of presenting the data that allows more of the results to be seen at once and provides additional insight, is a tabulated, statistical presentation. The antenna gains observed over the circular flight paths were analyzed to determine the rms variations from the mean. These variations are listed in Tables 5, 6, and 7 for antennas #5, #9, and #11 respectively, for the various elevation angles and frequencies. In interpreting these results, it should be noted that the maximum variations from mean are several times larger than the rms variations in many cases. Nonetheless, the rms variations provide a basis for comparison, in determining which conditions tend to produce the greatest azimuthal variations in the antenna patterns.

Table 5: Rms variation in gain observed over azimuth, for antenna #5, for various frequencies and elevation angles.

elevation	5.1 MHz	9.3 MHz	11.5 MHz	15.1 MHz	18.0 MHz
4.5°	1.2 dB	1.3	1.4	1.0	0.8
11° (cw)	0.9	1.1	1.1	0.8	0.7
11° (ccw)	0.9	1.2	1.2	0.8	0.7
18°	0.7	0.9	1.3	0.9	0.8
31°	0.6	0.6	1.2	1.1	1.0
49°	1.1	1.1	1.6	1.6	1.1

Table 6: Rms variation in gain observed over azimuth, for antenna #9, for various frequencies and elevation angles.

elevation	5.1 MHz	9.3 MHz	11.5 MHz	15.1 MHz	18.0 MHz
4.5°	1.4 dB	1.2	1.8	1.0	1.5
11° (cw)	0.7	1.2	1.6	1.0	1.5
11° (ccw)	0.8	1.2	1.8	1.0	1.6
18°	0.5	1.1	1.7	0.9	1.3
31°	0.7	0.9	1.7	1.1	1.4
49°	1.0	1.5	1.9	1.5	1.5

Table 7: Rms variation in gain observed over azimuth, for antenna #11, for various frequencies and elevation angles.

elevation	5.1 MHz	9.3 MHz	11.5 MHz	15.1 MHz	18.0 MHz
4.5°	1.6 dB	1.3	1.0	0.7	0.6
11° (cw)	0.8	1.0	0.8	0.5	0.8
11° (ccw)	0.9	1.0	1.0	0.6	0.8
18°	0.5	0.7	0.9	1.0	1.1
31°	0.6	0.7	1.1	0.9	0.8
49°	1.1	1.0	1.8	1.5	1.7

The results in Tables 5, 6 and 7 confirm the findings of the azimuthal gain plots based on fewer measurements.

Antenna #11, which is furthest-removed from other radiating structures, tends to have smaller azimuthal variations in gain than the other two antennas. Antenna #9, which is fairly close to the larger elements in the outer ring of the Pusher array, has the largest azimuthal variations in gain. These differences, which were previously noted in Section 6.2.2, suggest that the antenna patterns are being affected by interaction between elements.

At the lowest operating frequency, 5.1 MHz, the azimuthal rms gain variation shown in Tables 5, 6 and 7 is significantly greater at the lowest elevation angle (4.5°) than the other elevations. This is true for all three antennas. A similar but much weaker effect occurs at the next low-

est frequency (9.3 MHz). This effect is due to the ground feature inferred previously in Section 6.2.2, to extend outwards of 3 km and thus to contribute to the first Fresnel zones of the antennas at 4.5° elevation and 5.1-MHz and possibly 9.3-MHz frequencies, but not the other elevations and frequencies. The highest elevation angle (49°) likewise experiences larger rms gain variations, likely due to transmitting antenna orientation variations as discussed in Section 6.2. Apart from these differences, the rms variations in gain with azimuth do not show any obvious consistent differences with elevation angle, over the five frequencies measured.
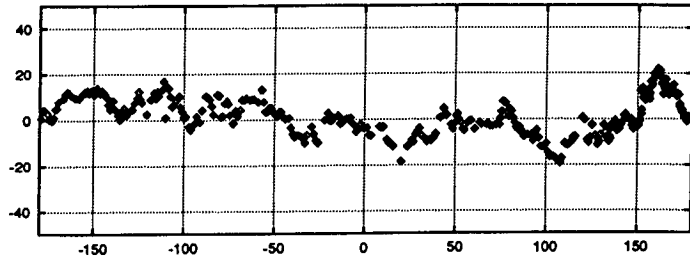
6.3 Relative Phase Patterns

The differential-GPS position error is less than 10 m, which corresponds to an absolute phase error of 60° at a 5.1-MHz operating frequency, and more at higher frequencies. Relative phase measurements are much more accurate. For instance, for the azimuthal runs at 11° elevation, a 10-m position error corresponds to at most a relative phase error of 1.3° between antennas #1 and #12, at 5.1 MHz. (Antenna #12 is the furthest removed from antenna #1, and thus will have the largest relative phase error due to position errors). At the highest frequency, 18.0 MHz, the corresponding maximum relative phase error is 4.7°. Thus the Xeledop should be capable of providing reasonably accurate relative phase measurements which suffice for applications such direction-finding and adaptive interference cancellation, but cannot provide absolute phase measurements. (It should be noted that the quoted errors are upper limits; most of the time the errors will be much less.)
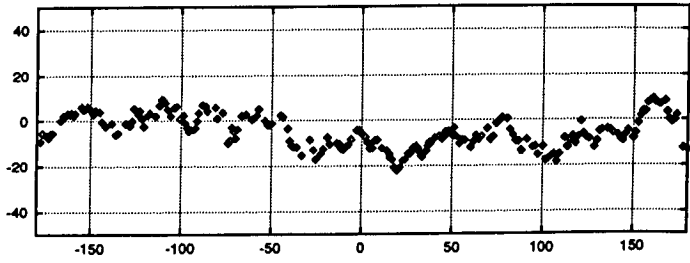
Figure 21 shows representative plots of the difference $\Delta\phi$ from spherical wavefront theory in the relative phase response between antennas #5 and #1, at 9.3 MHz, as a function of azimuth, for various elevation angles. The values of $\Delta\phi$ observed in this figure are a few degrees or more: substantially larger than the phase errors predicted from a 10-m position error. (For these antennas and this frequency, a position error of 10 m corresponds to a phase-difference error of at most 0.15°, 0.21°, 0.28°, 0.42°, and 0.55° for elevation angles of 4.5°, 11°, 18°, 31°, and 49° respectively.) The plots at all but the highest elevation angle are similar in the way $\Delta\phi$ varies over azimuth: variations from spherical theory $\Delta\phi$ are of the order of a few degrees, and occasionally reach 20°. At 49° elevation, the variations $\Delta\phi$ are substantially larger and show a markedly different azimuth dependence.

Similar plots, displaying $\Delta\phi$ for antennas #9 and #11 relative to antenna #1, are provided in Figures 22 and 23, respectively. These figures show a behaviour similar to that of Figure 21. The azimuthal variations in $\Delta\phi$ are similar for the four lower elevation angles of 4.5°, 11°, 18°, and 31°. As before, $\Delta\phi$ tends to be a few degrees most of the time, and occasionally increases to as much as 20° relative phase. The azimuthally-dependent variations in $\Delta\phi$ remain roughly the same for elevation angles between 4.5° and 31°. The azimuthal variations in $\Delta\phi$ at 49° eleva-
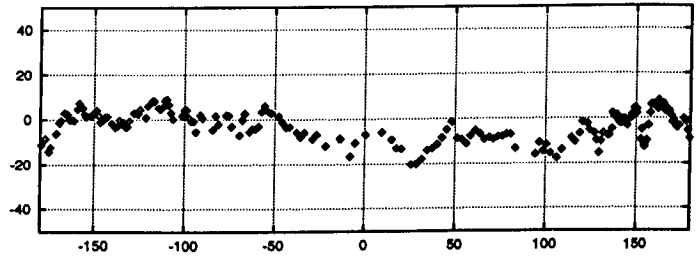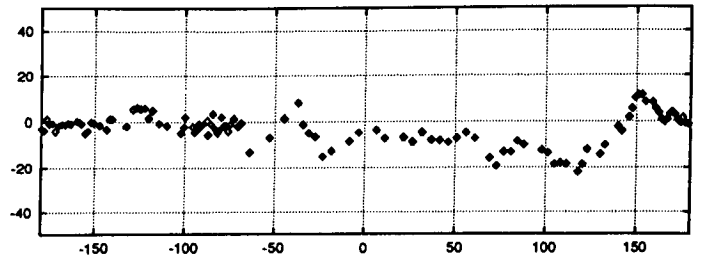
4.5 degrees
elevation

11 degrees
elevation

18 degrees
elevation

31 degrees
elevation

49 degrees
elevation
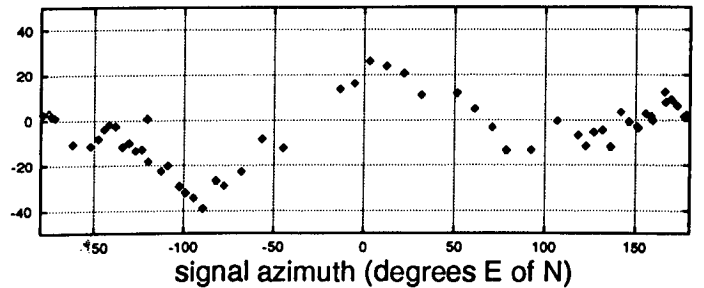
difference from theory in relative phase response Δφ of antennas 5 and 1 (degrees)

signal azimuth (degrees E of N)

Figure 21. Δφ for antennas #5 relative to #1at 9.3 MHz, plotted as a function of azimuth for various elevation angles.

33

4.5 degrees
elevation

11 degrees
elevation

18 degrees
elevation

31 degrees
elevation

49 degrees
elevation

Figure 22. Δφ for antenna #9 relative to #1 at 9.3 MHz, plotted as a function of azimuth for various elevation angles.
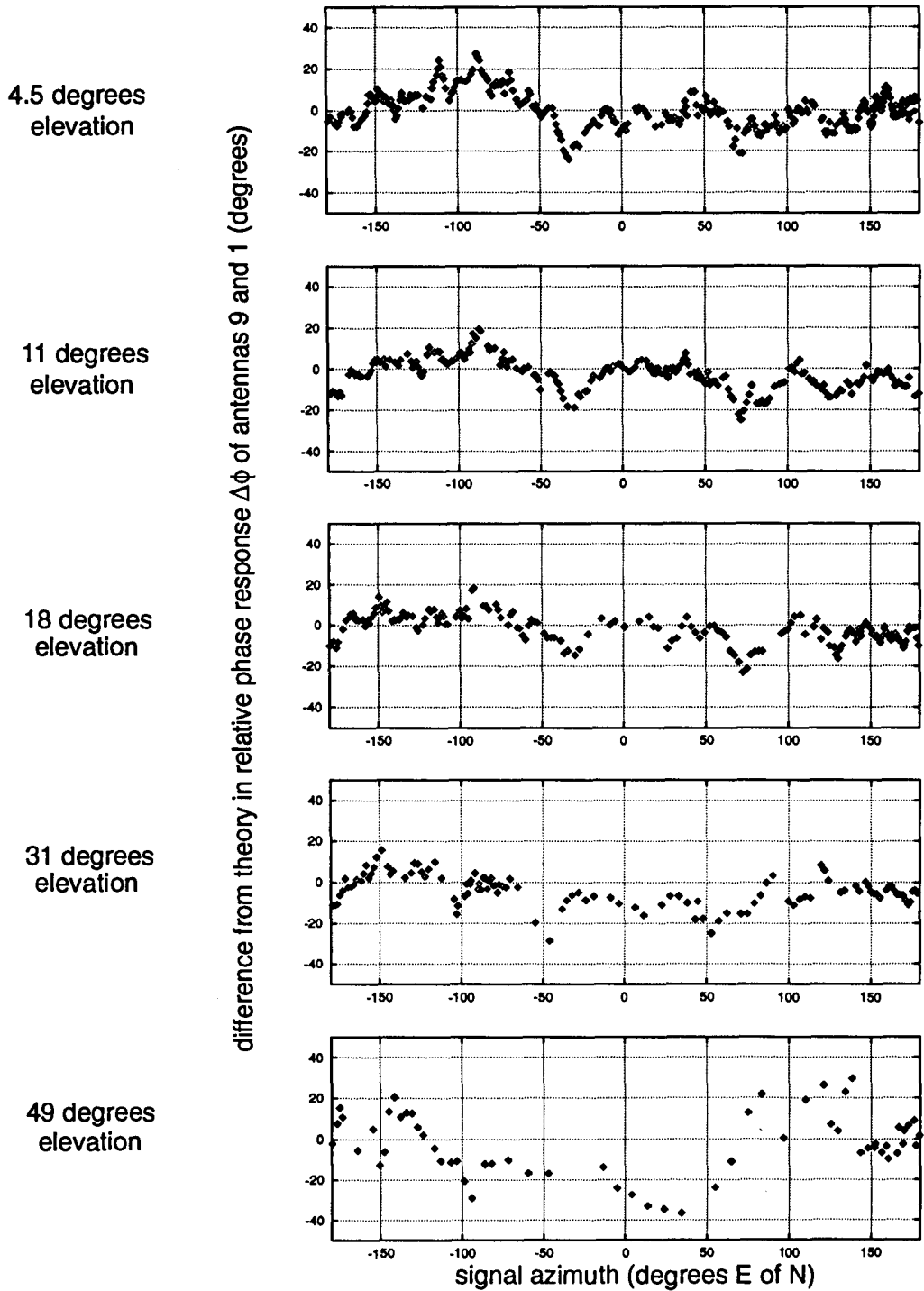
34

4.5 degrees
elevation

11 degrees
elevation

18 degrees
elevation

31 degrees
elevation

49 degrees
elevation

difference from theory in relative phase response Δφ of antennas 11 and 1 (degrees)
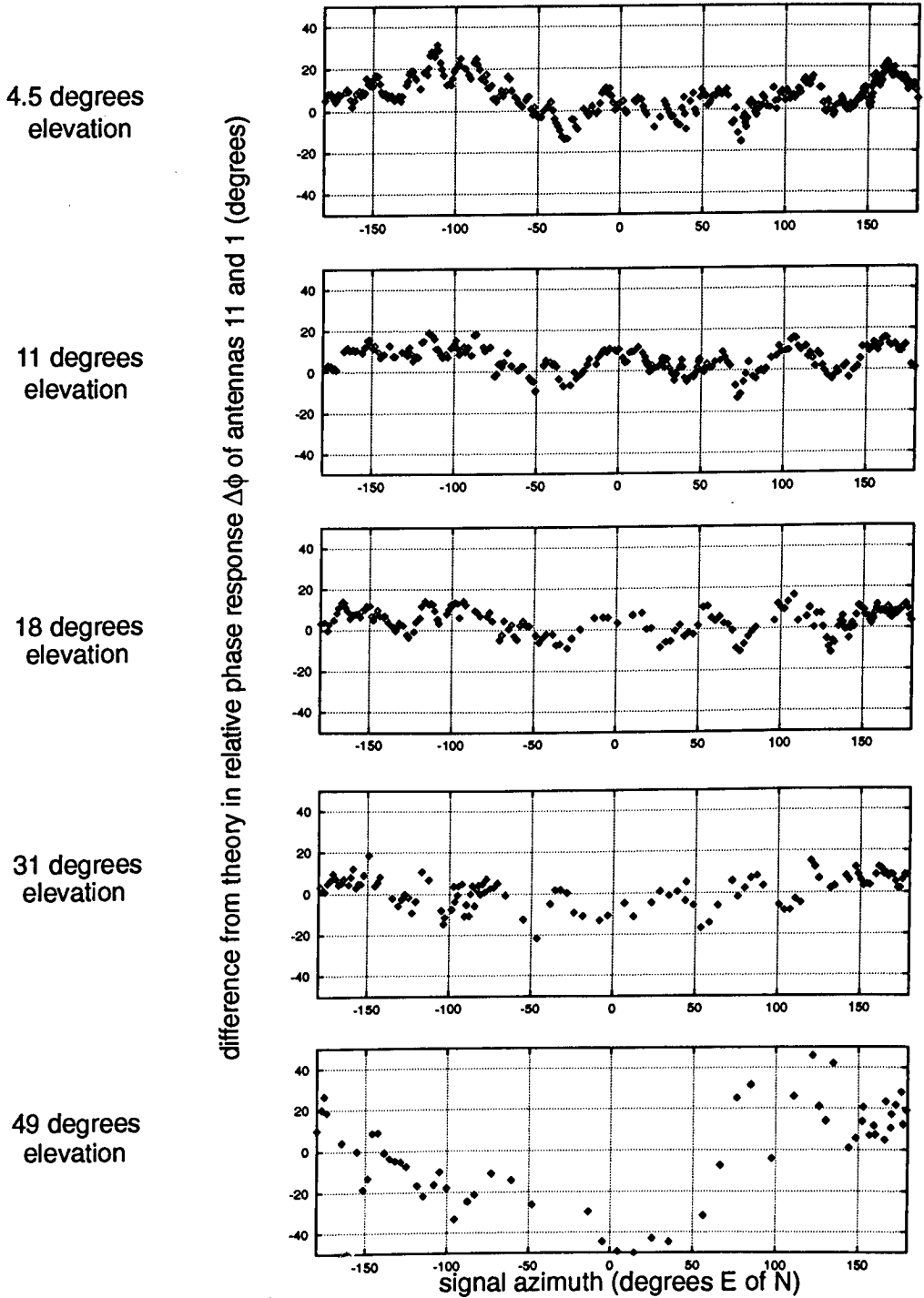
signal azimuth (degrees E of N)

Figure 23. Δφ for antenna #11 relative to #1 at 9.3 MHz, plotted as a function of azimuth for various elevation angles.

35

tion are much larger than those at the other (lower) elevations and do not show the same azimuthal dependence.

The 49° results may be dependent on the antenna separation, possibly suggesting an unexpectedly large transmitter position error. The relative phase responses for antenna #5 (a separation from antenna #1 of 40 m) differ from spherical wavefront values by as much as 30° to 40° at this elevation angle (Figure 21), as do the relative phase responses for antennas #9 (a separation of 95 m) (Figure 22). However, the relative phase responses for antennas #11 (a separation of 131 m) differ from the spherical wavefront values by as much as 50° (Figure 23). This issue is explored more thoroughly later in the report.

Observations at the other frequencies confirm the present findings, that the relative-phase results are consistent between different elevation angles with the dramatic exception of the highest elevation (49°) where the differences from theory vary differently with azimuth and are much larger.

The frequency dependence of the antenna phase measurements is illustrated in Figures 24, 25, and 26. These figures show the difference from theory in the phase response of antennas #5, #9, and #11 respectively, taken relative to antenna #1, for the five frequencies used in the pattern measurements. The 11°-elevation flight path measurements were used for these figures.

From Figures 24, 25, and 26, the values observed for $\Delta\phi$ for the three antennas can be seen to increase as the operating frequency is raised. Differences between the three antennas appear to dominate the azimuthal patterns at the 5.1-, 9.3-, and 11.5-MHz operating frequencies. Also, there is little similarity between these three frequencies in the observed azimuthal variations of $\Delta\phi$. At the two highest frequencies (15.1 and 18.0 MHz), a different behaviour is observed: the observed values of $\Delta\phi$ have a roughly similar azimuthal dependence, not only between the two frequencies but also between the three illustrated antennas. (The similarity between antennas in their relative phase behaviour at these frequencies does not necessarily indicate a common perturbing mechanism remote from the array; the values shown are taken relative to a common antenna (#1) whose own azimuthal phase dependence may well be the source of the similar azimuthal behaviour.)

One anomalous result is observed in Figures 24, 25, and 26. Generally, the values of $\Delta\phi$ vary with azimuth about an average near 0°. A single exception to this is seen at 5.1 MHz in Figure 26 for antenna #11. The observed large offset in this case (approximately -30°) is likely caused by an error in the channel-calibration phase correction for antenna #11 at 5.1 MHz. The same offset is observed for this antenna and frequency for the flight paths flown at other elevations, in agreement with the interpretation.

Figure 24. Δφ for antenna #5 relative to #1 at 11 degrees elevation, plotted as a function of azimuth for five operating frequencies.

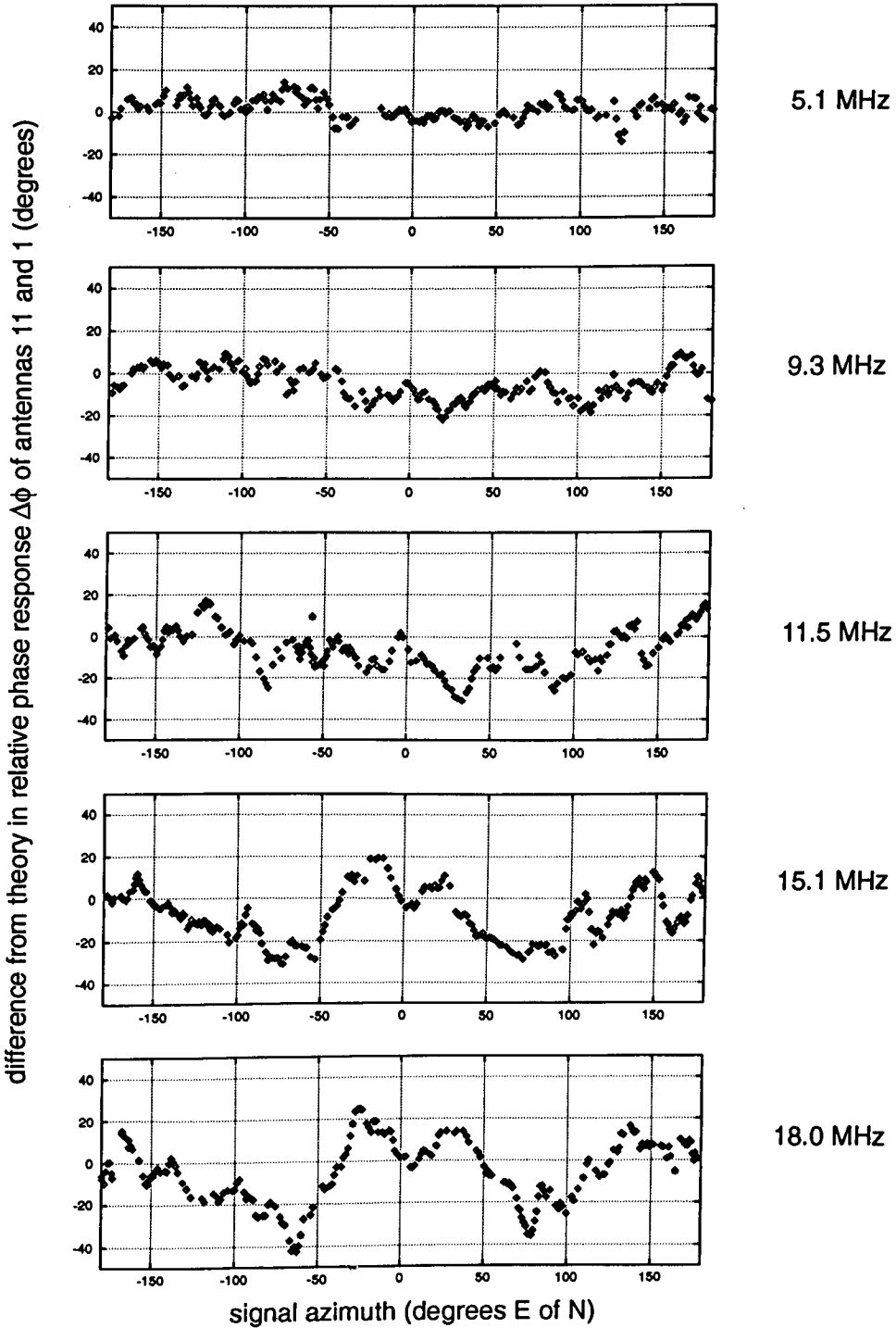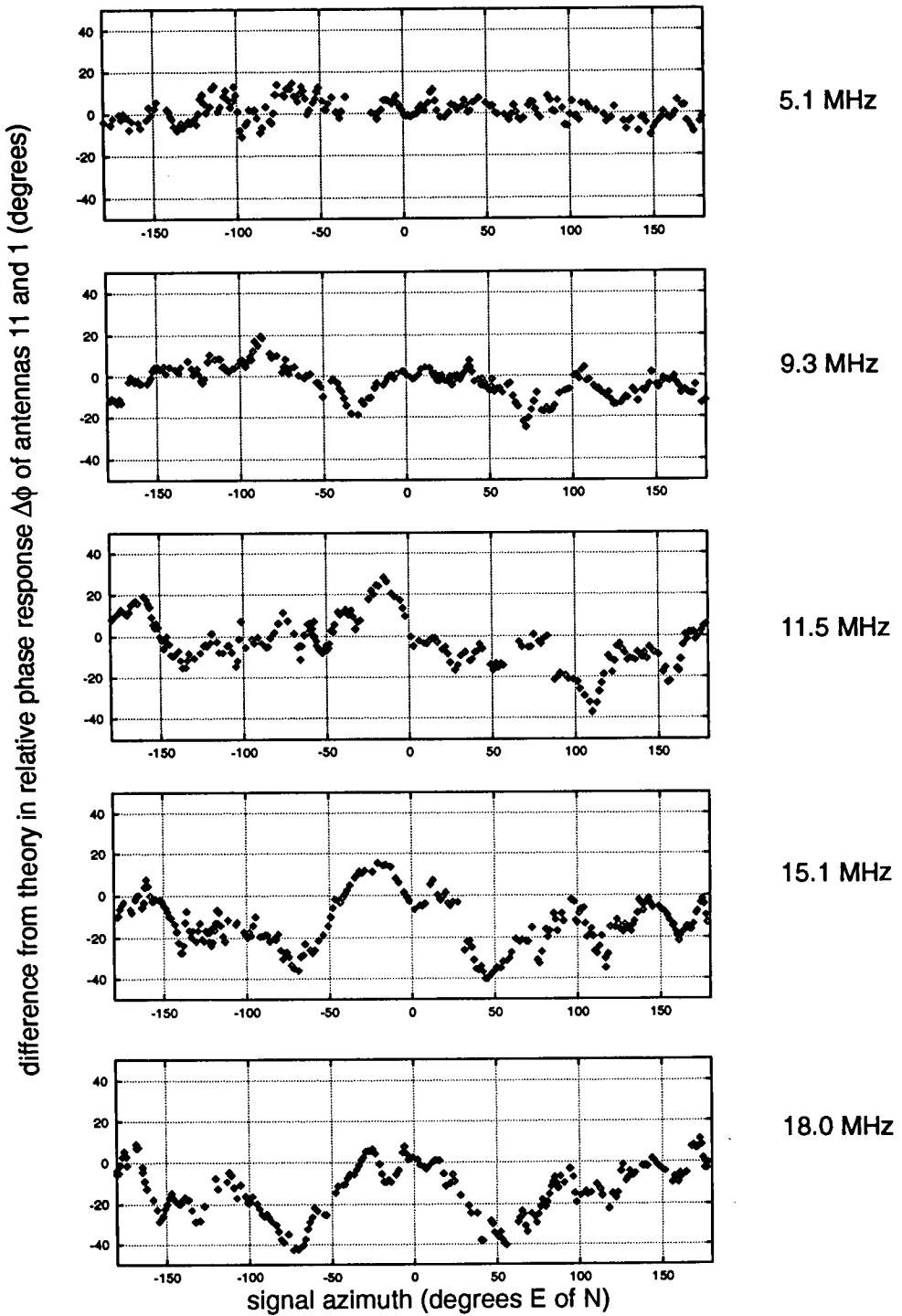*Figure 25.* Δφ *for antenna #9 relative to #1 at 11 degrees elevation, plotted as a function of azimuth for five operating frequencies.*

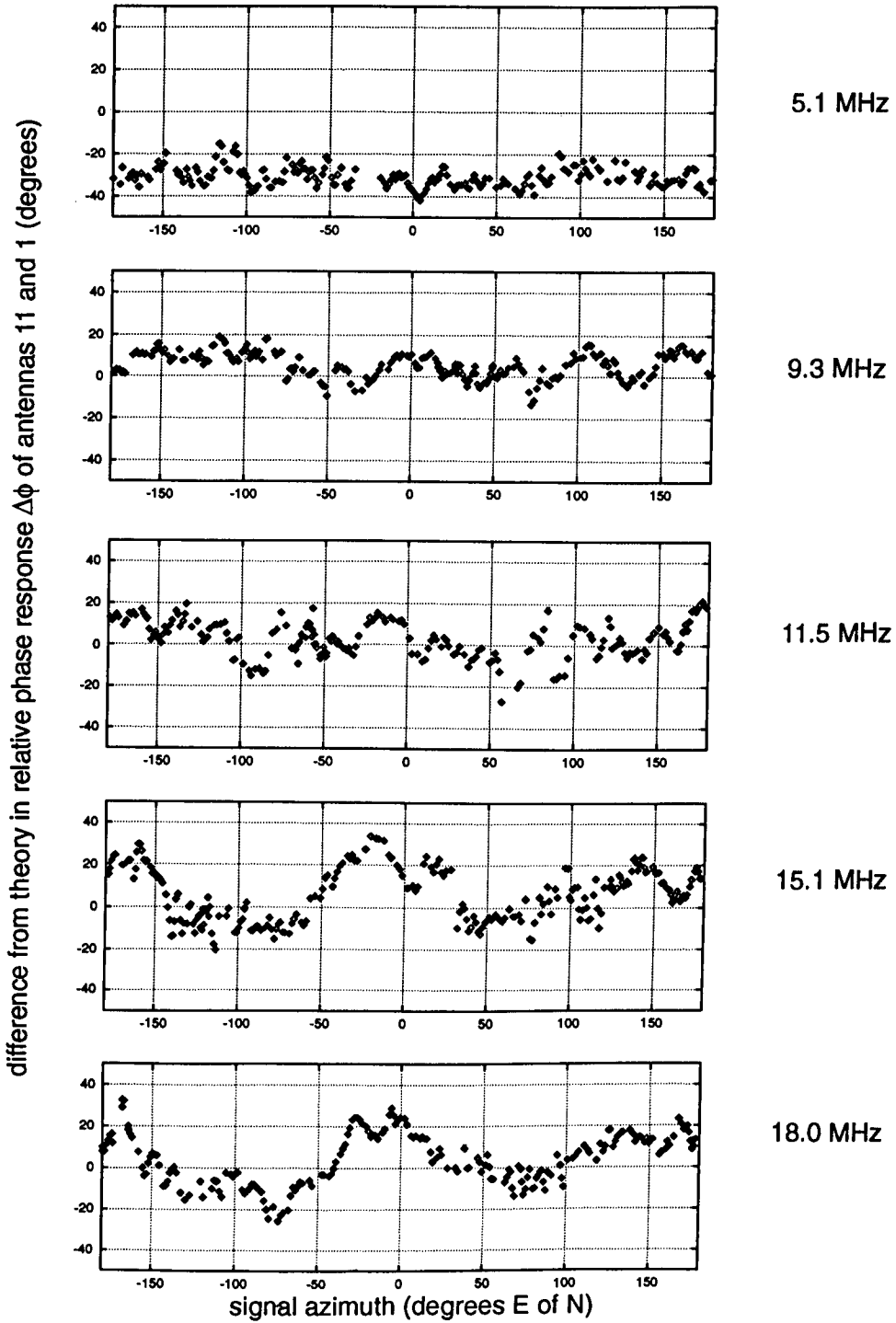*Figure 26. Δφ for antenna #11 relative to #1 at 11 degrees elevation, plotted as a function of azimuth for five operating frequencies.*

A check on the effect of position errors on the relative phase measurements can be made by comparing the results of the two runs made over the same flight path, at 11° elevation, in the clockwise and counterclockwise directions. Figure 27 shows the result for antenna #5 taken at 9.3 MHz. As can be seen from this figure, the two sets of measurements are in good agreement. Small differences exist, but they are much smaller than the azimuthal variations themselves.
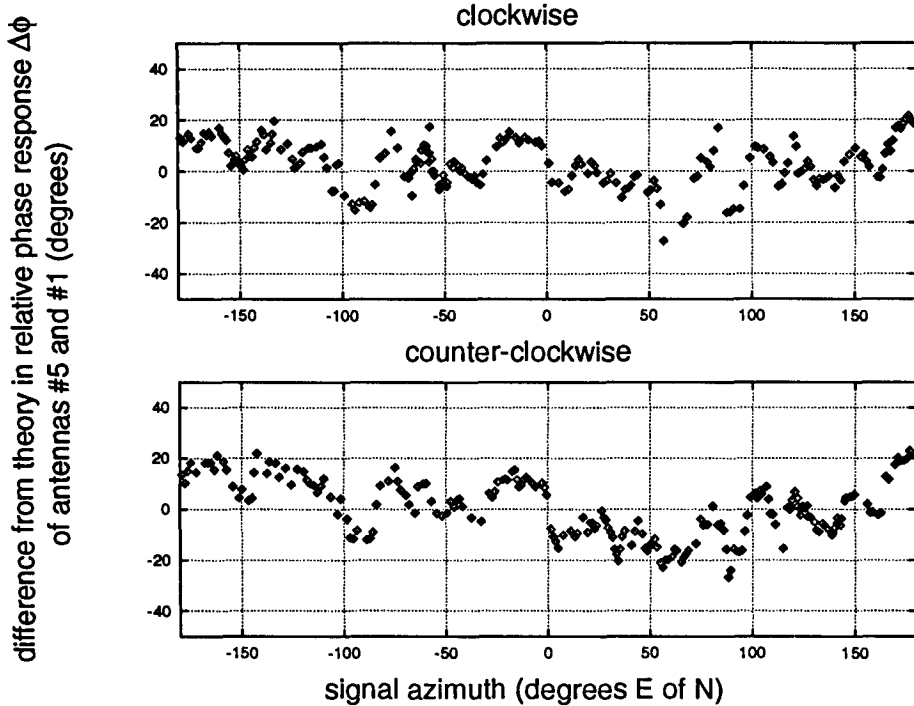

Figure 27. Δφ for antenna #5 relative to #1, at 9.3 MHz operating frequency and 11 degrees elevation angle, obtained as a function of azimuth from clockwise and counterclockwise flight paths.

Table 8 summarizes the result for all antennas and frequencies, showing the rms variations in the difference from theory in the relative phase response Δφ and the corresponding rms measurement error deduced from a differences seen between the clockwise and counterclockwise runs, for all antennas and operating frequencies. From this table, it is clear that the errors introduced by the measurement technique (position and otherwise) are much less than the observed differences from theory in the relative phase.

Other features of the relative phase response can also be seen in Table 8. Firstly, there is only a very small dependence of the difference from theory Δφ on antenna separation: the smallest antenna separation (antenna #2) appears to deviate less from theory in its relative phase response than the others, which do not differ between themselves appreciably. The difference from theory does increase significantly with frequency, although not quite proportionally.

40

Table 8: Rms differences from mean in the difference from theory in phase response Δφ relative to antenna #1, as measured for each antenna and frequency at 11° elevation angle, and the corresponding rms measurement error (in brackets) deduced from a comparison of clockwise and counterclockwise runs.

antenna	5.1 MHz	9.3 MHz	11.5 MHz	15.1 MHz	18.0 MHz
2	2.1° (0.5°)	5.3 (1.2)	7.6 (1.0)	8.4 (1.0)	9.9 (1.4)
3	4.0 (1.1)	6.8 (1.3)	8.2 (1.2)	11.5 (0.9)	13.1 (1.4)
4	4.4 (1.2)	7.0 (1.5)	8.4 (1.4)	11.9 (1.1)	13.6 (1.6)
5	4.7 (1.2)	7.1 (1.6)	10.0 (1.8)	12.1 (1.3)	15.0 (2.2)
6	4.6 (1.3)	10.4 1.9)	10.8 (1.9)	9.5 (1.5)	11.8 (2.3)
7	4.9 (1.3)	7.5 (1.8)	9.4 (1.8)	13.4 (1.3)	16.4 (1.9)
8	4.7 (1.3)	7.1 (1.8)	8.8 (1.8)	14.8 (1.3)	15.4 (1.8)
9	5.2 (1.6)	8.2 (2.7)	12.4 (2.9)	12.3 (2.6)	12.9 (2.9)
10	6.7 (1.6)	6.3 (2.4)	12.1 (3.7)	10.1 (2.7)	12.6 (3.4)
11	4.9 (1.6)	7.2 (3.2)	10.0 (4.0)	12.7 (3.5)	12.4 (3.8)
12	6.9 (2.2)	7.8 (3.2)	9.5 (4.5)	9.7 (3.5)	10.0 (4.4)

The measurement-related errors shown in Table 8, unlike the differences from theory Δφ, do show a strong dependence upon antenna separation as well as frequency, consistent with what might be expected if the errors are primarily due to position uncertainties. Making the assumptions that the largest relative phase measurement errors (recorded for antenna #12 which has the largest separation) are due entirely to position errors, and that these position errors do not vary appreciably from flight to flight, the relative phase measurements expected for other elevations can be calculated. Using the 11.5-MHz measurement error given in Table 8 for 11° elevation, relative phase measurement errors of 3.2°, 6.1°, 9.2°, and 11.9° are predicted for 4.5°, 18°, 31°, and 49° elevations respectively, for antenna #12 at this frequency. (The phase error measurement for antenna #12 of 11.5 MHz corresponds to the largest position error estimate over all frequencies and antennas, and thus provides an upper limit to the relative phase measurements errors calculated for other elevations. The corresponding position error estimate is 16 m, somewhat greater than the 10 m differential-GPS maximum position error; the greater error may be caused by uncertainties in the exact position of the transmitter relative to the aircraft.)

The observed rms variations with azimuth, in Δφ for antenna #12 relative to #1 at 11.5 MHz (8.6°, 9.5°, 9.8°, and 32.1°, for 4.5°, 18°, 31°, and 49° elevations, respectively) are for the most part, substantially higher than the inferred relative phase measurement errors.

Tables 9,10 and 11 show the rms variations with azimuth, in the difference from theory in the relative phase $\Delta\phi$ of antennas #5, #9, and #11 respectively, as a function of elevation angle and frequency. Also included (in brackets) are the corresponding relative phase measurement rms errors inferred from the clockwise/counterclockwise flight path differences observed at 11° elevation, on the assumption that these differences are due to a statistically constant rms position error. The behaviour noted in Table 7 is also apparent in Tables 9, 10 and 11.

Table 9: Rms difference from mean, in $\Delta\phi$ for antenna #5 relative to #1, and the corresponding measurement error (in brackets) inferred from the observed clockwise/ counterclockwise differences in relative phase observed for antenna #5 at 11° elevation, for various elevation angles and frequencies.

elevation	5.1 MHz	9.3 MHz	11.5 MHz	15.1 MHz	18.0 MHz
4.5°	4.4° (0.9°)	8.7 (1.1)	8.7 (1.3)	11.8 (0.9)	14.3 (1.6)
11°	4.7 (1.2)	7.1 (1.6)	10.0 (1.8)	12.1 (1.3)	15.0 (2.2)
18°	4.6 (1.6)	6.5 (2.2)	8.6 (2.4)	12.9 (1.7)	15.3 (3.0)
31°	5.0 (2.4)	6.7 (3.3)	10.4 (3.7)	12.9 (2.7)	11.1 (4.5)
49°	6.8 (3.2)	14.1 (4.2)	13.5 (4.8)	14.0 (3.4)	14.6 (5.8)

Table 10: Rms difference from mean, in $\Delta\phi$ for antenna #9 relative to #1, and the corresponding measurement error (in brackets) inferred from the observed clockwise/ counterclockwise differences in relative phase observed for antenna #9 at 11° elevation, for various elevation angles and frequencies.

elevation	5.1 MHz	9.3 MHz	11.5 MHz	15.1 MHz	18.0 MHz
4.5°	5.5° (1.1°)	8.5 (1.9)	13.0 (2.1)	11.9 (1.9)	12.6 (2.1)
11°	5.2 (1.6)	8.2 (2.7)	12.4 (2.9)	12.3 (2.6)	12.9 (2.9)
18°	5.7 (2.2)	6.9 (3.6)	10.9 (3.9)	10.2 (3.5)	11.2 (3.9)
31°	5.0 (3.3)	7.6 (5.5)	9.8 (5.9)	10.2 (5.3)	10.2 (5.9)
49°	7.9 (4.2)	15.2 (7.1)	25.5 (7.7)	23.1 (6.9)	31.9 (7.7)

Table 11: Rms difference from mean, in the Δφ for antenna #11 relative to #1, and the corresponding measurement error (in brackets) inferred from the observed clockwise/ counterclockwise differences in relative phase observed for antenna #11 at 11° elevation, for various elevation angles and frequencies.

elevation	5.1 MHz	9.3 MHz	11.5 MHz	15.1 MHz	18.0 MHz
4.5°	5.7° (1.1°)	8.2 (2.3)	8.3 (2.9)	12.0 (2.5)	11.7 (2.7)
11°	4.9 (1.6)	7.1 (3.2)	10.0 (4.0)	12.6 (3.5)	12.4 (3.8)
18°	4.6 (2.2)	5.9 (4.3)	9.1 (5.4)	11.2 (4.7)	12.6 (5.1)
31°	4.1 (3.3)	7.4 (6.5)	10.1 (8.2)	14.0 (7.1)	13.9 (7.7)
49°	11.7 (4.2)	23.8 (8.5)	29.7 (10.6)	36.4 (9.3)	45.3 (9.3)

The inferred measurement errors are substantially smaller than the observed rms values of Δφ for each of the three representative antennas #5, #9, and #11, at all elevation angles and frequencies. The observed rms values of Δφ are approximately the same at the four lower elevation angles, 4.5 to 31°. At the highest elevation angle (49°), the rms values increase substantially.

The much higher differences Δφ from the spherical-wavefront value in the observed relative phases at the 49° elevation angle suggests that the signals coupled into the antennas from neighbouring structures may play a relatively larger role than at the lower elevation angles. At the higher angle, the direct-signal responses of the vertical antenna elements are starting to fall off significantly, so any non-vertical conducting structures could have a much more significant effect in coupling signals to the vertical elements. Such an effect would be felt most strongly in the phase patterns, since the phases, more so than the amplitudes, can be altered significantly by the addition of lower-amplitude signals re-radiated from nearby structures.

7.0 CONCLUSIONS

7.1 Xeledop Pattern Measurement System

The Xeledop transmitting system, on the basis of the test measurements, has been shown to be capable of providing accurate antenna pattern measurements of both gain and relative phase, at elevation angles between 4.5° and 45°. Typical measurement errors are of the order of 0.5 dB in gain, and 3° in relative phase.

The pattern measurements are restricted to a minimum elevation angle of approximately 4.5°. This restriction is caused by the mismatch between the first Fresnel zone and thus ground

contributing to the antenna gain and phase response that occurs at low elevation angles between far-distant skywave signals and Xeledop transmitter signals coming from a closer distance. It is important to fly the transmitter as far away as possible for these measurements, recognising that this distance is limited in practice for any given elevation by the maximum attainable aircraft height.

At higher elevation angles, variations in the transmitting antenna orientation cause corresponding variations in the signal power radiated toward the antennas being calibrated, and resultant errors in estimated antenna gain. These errors become greater with increasing elevation and represent a serious limitation above 45° elevation.

Xeledop transmitter position errors likewise are more serious in their effect on relative phase at the higher elevation angles, where the distances from the transmitter to the array under calibration are necessarily less. Position errors are caused in part by the limitations of the differential GPS technique, and possibly in part by uncertainties in the position of the transmitter relative to the aircraft. The position errors were estimated to be at most 16 m for the 11°-elevation flight paths (7-km turning radius), but they might be larger for the higher-elevation (smaller turning radius) flight paths.

In order to specify the measurement errors more fully, future Xeledop pattern measurements should include clockwise and counterclockwise flight paths for the more error-prone higher elevation angles. Consideration should also be given to flying radial flight paths twice to check the repeatability of the elevation pattern measurements as well.

Care needs to be taken in future measurements to ensure that the times recorded for the GPS position data and the corresponding received signal data are synchronous.

7.2 Antenna Array

The antenna array element patterns were found to be substantially different from those expected on the basis of simple spherical wavefronts propagating over uniform earth. The antenna patterns differed from circular by several dB, and the relative phase responses differed from those expected for spherical wavefronts by a few degrees, and sometimes as much as 40° or even 50°.

The element patterns were seen to be influenced by neighbouring structures including both the other elements and local features external to the array. They were also influenced, notably at the lower elevation angles and frequencies, by more distant anomalous ground features.

The antenna gains varied most with azimuth at the lowest elevation angle (4.5°) where relatively distant ground anomalies had the greatest effect. At higher elevation angles, localized

features, including nearby conducting structures and possibly small-scale ground features, had a predominant effect on the observed antenna gains.

The relative phase response of the antennas showed a strong dependence on operating frequency, differing from the spherical-wavefront values by amounts that increased with frequency in a slightly less than proportional manner. The dependence on antenna separation was less clear: smaller differences from the spherical-wavefront value were observed for the smallest separation (antenna #2 relative to #1, 6.5 m) than for the other separations (> 19 m), which showed no consistent variation between themselves. Likewise, there was little dependence on elevation angle in the relative phase response, for elevations from 4.5° to 31°. The relative phase response did increase significantly in its difference from the spherical-wavefront value, at the highest elevation angle (49°). This increase could not be explained by the greater effects of transmitter position errors, and may have been due to the reduced sensitivity of the vertical antennas to direct signals and the resulting greater role of nearby non-vertical conducting structures in coupling signals into the (vertical) antennas, at high elevation angles.

In order to help establish to what extent these antenna patterns can be predicted, it is recommended that numerical antenna modelling of the current array be conducted (using the numerical electromagnetic computation software NEC), thereby obtaining predicted antenna gains and relative phase responses that can be compared with the measured values. (Modelling studies are currently being conducted under contract.)

It is also recommended that simulation studies be conducted, to establish the effects the measured antenna gain and relative phase variations have on direction-finding accuracy in the presence of one or more signals, and the extent to which accuracy can be improved through the use of NEC modelling, and through actual pattern measurements.

ACKNOWLEDGEMENTS

REFERENCES

[1]   R. W. Jenkins, *The Effect of Snow on Antenna Radiation Patterns: A Presentation of Results*, IEEE Trans. Antennas and Propagation, **AP-21**, 5, 722-725, 1973.

[2]   G.E. Moss, N. Muirhead, and R.W. Jenkins, *The Use of Multiple-Element Beverage Antenna Arrays for HF Transmissions*, CRC Report **1318** ,1978.

[3]   *Xeledop Antenna Measurement System Using DGPS to Track Aircraft*, Petrie Telecommunications Ltd. Report **280994**, performed under CRC contract 36001-3-3545, 1994.

[4]   P. Soble, personal communication, 1995.

[5]   L.E. Petrie, personal communication, 1995.

DOCUMENT CONTROL DATA

(Security classification of title, body of abstract and indexing annotation must be entered when the overall document is classified)

1. ORIGINATOR (the name and address of the organization preparing the document. Organizations for whom the document was prepared, e.g. Establishment sponsoring a contractor's report, or tasking agency, are entered in section 8.) Communications Research Centre 3701 Carling Avenue, P.O. Box 11490, Station H OTTAWA, Ontario K2H 8S2	2. SECURITY CLASSIFICATION (overall security classification of the document. including special warning terms if applicable) UNCLASSIFIED

3. TITLE (the complete document title as indicated on the title page. Its classification should be indicated by the appropriate abbreviation (S,C or U) in parentheses after the title.)

Antenna Amplitude and Phase Pattern Measurements Using an Aircraft-Towed Transmitter (U)

4. AUTHORS (Last name, first name, middle initial)

Jenkins, Robert, W.

5. DATE OF PUBLICATION (month and year of publication of document) September 1995	6a. NO. OF PAGES (total containing information. Include Annexes, Appendices, etc.) 54	6b. NO. OF REFS (total cited in document)

7. DESCRIPTIVE NOTES (the category of the document, e.g. technical report, technical note or memorandum. If appropriate, enter the type of report, e.g. interim, progress, summary, annual or final. Give the inclusive dates when a specific reporting period is covered.)

CRC Report

8. SPONSORING ACTIVITY (the name of the department project office or laboratory sponsoring the research and development. Include the address.) DEFENCE RESEARCH ESTABLISHMENT OTTAWA (DREO)
        3701 Carling Avenue, Bldg. 29
        OTTAWA, Ontario   K1A 0Z4

9a. PROJECT OR GRANT NO. (if appropriate, the applicable research and development project or grant number under which the document was written. Please specify whether project or grant) 04160	9b. CONTRACT NO. (if appropriate, the applicable number under which the document was written)
10a. ORIGINATOR'S DOCUMENT NUMBER (the official document number by which the document is identified by the originating activity. This number must be unique to this document.) CRC-95-003	10b. OTHER DOCUMENT NOS. (Any other numbers which may be assigned this document either by the originator or by the sponsor) DREO DRP 95-314

11. DOCUMENT AVAILABILITY (any limitations on further dissemination of the document, other than those imposed by security classification)

(X) Unlimited distribution
( ) Distribution limited to defence departments and defence contractors; further distribution only as approved
( ) Distribution limited to defence departments and Canadian defence contractors; further distribution only as approved
( ) Distribution limited to government departments and agencies; further distribution only as approved
( ) Distribution limited to defence departments; further distribution only as approved
( ) Other (please specify):

12. DOCUMENT ANNOUNCEMENT (any limitation to the bibliographic announcement of this document. This will normally correspond to the Document Availabilty (11). However, where further distribution (beyond the audience specified in 11) is possible, a wider announcement audience may be selected.)

13. ABSTRACT (a brief and factual summary of the document. It may also appear elsewhere in the body of the document itself. It is highly desirable that the abstract of classified documents be unclassified. Each paragraph of the abstract shall begin with an indication of the security classification of the information in the paragraph (unless the document itself is unclassified) represented as (S), (C), or (U). It is not necessary to include here abstracts in both offical languages unless the text is bilingual).

A previously built antenna pattern measurement system, consisting of a short transmitting dipole and self-contained transmitter towed behind a light aircraft, was modified to permit measurements of both antenna gain and relative phase. A differential GPS positioning system was added to provide the necessary accurate transmitter position information. The pattern measurement system is intended for calibrating HF antenna arrays used in direction-finding and other applications requiring knowledge of the array manifold.

The system was used to provide element pattern measurements on an HF antenna array located near Ottawa. The measurements provided a measure of the accuracy of the pattern measurement technique and its limits of applicability. The element patterns were observed to be affected by interactions between neighbouring elements and other localized features and, to a lesser extent, by larger-scale more distant ground or topographical effects.

14. KEYWORDS, DESCRIPTORS or IDENTIFIERS (technically meaningful terms or short phrases that characterize a document and could be helpful in cataloguing the document. They should be selected so that no security classification is required. Identifiers, such as equipment model designation, trade name, military project code name, geographic location may also be included. If possible keywords should be selected from a published thesaurus. e.g. Thesaurus of Engineering and Scientific Terms (TEST) and that thesaurus-identified. If it is not possible to select indexing terms which are Unclassified, the classification of each should be indicated as with the title.)

    pattern measurement
    dipole
    transmitter
    antenna array

Date Due

MAR 10 1999			

BRODART, CO.   Cat. No. 23-233-003   Printed in U.S.A.